RESEARCH REPORT

VTT-R-01157-10

Optimization tools for steel portal frames - Design and optimization methods

Authors: Petr Hradil, Matti Mielonen, Ludovic Fülöp

Confidentiality: Confidential

Public after closing the project (July 2010).

Report's title	
Optimization tools for steel portal frames - Design and optimization methods	
Customer, contact person, address Commission of the European Communities	Order reference RFS-PR-06054
Project name Prefabricated steel structures for low-rise buildings in seismic areas	Project number/Short name 12596/PRECASTEEL
Author(s) Petr Hradil, Matti Mielonen, Ludovic Fülöp	Pages 57 p.
Keywords steel, portal frame design, optimization, software benchmarking	Report identification code VTT-R-01157-10

Summary

The document presents portal frame design, and optimization results, obtained using two software tools developed at VTT. Both tools use analytical methods from Eurocode 3 (EN 1993-1-1 [7]) for design, and genetic algorithms for optimization. The tool developed for Abaqus (AP-Frame) models the frame with "Shell" type finite elements for out-of-plane stability calculations, while in the Excel tool (EV-Frame) stability is calculated at the level of members using analytical expressions of critical loads.

Two types of portal frames analysed. Hot-rolled frames are composed of rolled HE and IPE sections, with welded haunch on the beam. The second group are tapered frames, welded from steel plates.

Two analytical methods can be used in Abaqus tool (AP-Frame) to design the frames: General method (GMA) and global non-linear analysis using initial imperfections (GMNIA). The third method - member checks using interaction formulae - is included in Excel tool (EV-Frame). Both programs use genetic algorithms as optimization engine, with several possibilities of selection, crossover, and mutation methods.

In this report we describe a few calculation examples and optimization runs carried out with the software tools. Some of these calculations were use for the benchmarking of the software tools, while others were produced for the PRECASTEEL project. The study shows that, using the general method for design, one can achieve results with acceptable level of conservativeness and in reasonable time.

Public after closing the project (July 2010).

Confidentiality	Confidential

Espoo 24.5.2010

Written by	Reviewed by	Accepted by
Petr Hradil Research Scientist	Ludovic Fülöp Senior Research Scientist	Eila Lehmus Technology Manager

VTT's contact address
P.O. Box 1000, FI-02044 VTT, Finland

Distribution (customer and VTT)

Customer (Partners of EU-RFCS project PRECSATEEL):	(1pdf copy each)
VTT/Register Office:	(1 copy)

Preface

The research report describes the software tools, for analysis and optimization of steel portal frames, developed in VTT Research Centre of Finland for the PRECASTEEL project.

The tools are capable of automatic model creation, results evaluation and genetic algorithm optimization, and they are using an independent calculation core for finite element analysis.

EV-Frame is programmed as Microsoft Excel script, with open source finite element calculation [12] under GPL - general public license. AP-Frame is programmed in Python, using Abaqus commercial or academic licenses for numerical calculations. Detailed description of all required inputs and produced outputs is included in this report. The most important methods and objects of the code are also explained.

Two types of portal frames are considered in the analysis. Hot-rolled frames are composed of rolled HE and IPE sections with welded haunch on the beam. Those frames are usually fixed at the base. The second group covers tapered frames, fabricated from steel plates, which are usually pinned at the base.

Two design methods can be used in the Abaqus tool (AP-Frame): General method with overall out-of-plane reduction factor (GMA), and global non-linear analysis using initial imperfections (GMNIA). The third method - member checks using member slenderness and interaction formulae (IFM) - is included in Excel tool (EV-Frame). Both programs use genetic algorithms with several possible selection, crossover, and mutation methods.

Results presented in this study show the difference between GMA and GMNIA used in the Abaqus tool (AP-Frame), and the calculation of the frames with beam model, using CCS INSTANT software, and reduction factors approach for stability. CCS INSTANT was used for preliminary design of several frame configurations, performed by the University of Thessaly [11].

Results from optimization of hot-rolled frames, with EU profiles, are also compared with previous optimizations of similar frames [13]. The study shows that using GMA, we can achieve reliable results with acceptable level of conservativeness in a reasonable time.

Espoo 24.5.2010

Authors

Abbreviations

CAE	computer aided engineering
CS	cross-section
EC	Eurocode
FB	flexural buckling
FE	finite element
FEM	finite element method
GA	genetic algorithm
GMA	general method
GMNIA	analysis of the geometrically and materially nonlinear structure, including effects of initial imperfections
GNLA	global non-linear analysis
HR	hot-rolled
IFM	analysis method based on interaction formulae
LBA	linear eigenvalue (bifurcation) analysis
LTB	lateral torsional buckling
SLS	serviceability limit state
TB	torsional buckling
TFB	torsional flexural buckling
ULS	ultimate limit state
WT	welded-tapered
XML	Extensible Markup Language

Symbols

α_{cr}	critical multiplier of the loads (in-plane buckling)
$\alpha_{cr,op}$	critical multiplier of the loads (out-of-plane buckling)
$\alpha_{ult,k}$	minimum load amplifier of the design loads to reach the characteristic resistance
α_m, α_n	coefficients of variable cross-sections (Šapalas et al [2])
γ_G, γ_Q	partial safety factors for loading
γ_{M0}, γ_{M1}	partial safety factors for material
$\overline{\lambda}_y$, $\overline{\lambda}_z$	non-dimensional slenderness (“y” axis and “z” axis)
$\overline{\lambda}_{op}$	overall out-of-plane non-dimensional slenderness
χ_y, χ_z	buckling reduction factor (“y” axis and “z” axis)
χ_{op}	overall out-of-plane buckling reduction factor
ψ_0, ψ_2	combination factors
a	distance between two lateral supports (purlins or side rails)
$e_{z,\max}$	max. eccentricity of lateral support from the shear centre of the CS
$e_{z,\min}$	min. eccentricity of lateral support from the shear centre of the CS
f_y	yield stress
i_0	polar radius of gyration
k_z	effective length factor considering weak axis end-support conditions (k_z = 1 for pinned-pinned, k_z = 0.5 for fixed-fixed, k_z = 0.7 for pinned-fixed)
k_w	effective length factor considering end warping support (k_w=1 for no warping support, k_w = 0.5 for both end warping support)
z_g	load position (z-distance between load and shear center)
A	gross cross-section area
A_f	second order amplification factor
C_1, C_2	moment gradient factors
C_{my}	equivalent moment factors for FB
C_{mLT}	equivalent moment factors for LTB
E	Young’s modulus of elasticity
F_1	unit force
G	shear modulus
I_t	torsional constant
I_w	warping constant
$I_{y,\max}$, $I_{z,\max}$	strong/”y” and weak/”z” axis second moment of area at the large member cross-section
$I_{y,\min}$, $I_{z,\min}$	strong/”y” and weak/”z” axis second moment of area at the small member cross-section
K_{lat}	lateral (horizontal) stiffness of the frame
L	length of member

L_h	(horizontal) length of the haunch
$L_{cr,y}$, $L_{cr,z}$	critical lengths for strong/"y" and weak/"z" axis FB
N_{Ed}	design axial forces
N_{Rk}	characteristic resistance in compression
M_{cr}	critical bending moment
M_{eq}	earthquake mass
$M_{y,Ed}$	design bending moment to major/"y" axis bending moment
$M_{y,Ed,1}$ to $M_{y,Ed,5}$ - $M_{y,Ed}$	in quarter points along the length of the member
$M_{y,Rk}$	bending resistance (elastic or plastic depending on design method) to "y"/major axis
$S_d(T)$	the ordinate of the design spectrum for seismic calculation
T	fundamental period of vibration
$V_{z,Ed}$	shear force in "z" direction
$V_{z,Rk}$	shear resistance in "z" direction
Δ_1	deflection caused by unit force

Contents

1 Frame configurations

Design and optimization procedures were developed in order to analyze two portal frame configurations: frames made of hot rolled profiles (HR frames), and welded tapered frames (WT frames).

Hot-rolled (HR) frames with haunches on rafters are typically built with a fixed base, in order to decreases the overall steel consumption; however, designer has to keep in mind the increased demands on substructure and foundations.

On the other hand WT frames are typically pinned at the base. In these frames, the variation of column and rafter heights is made to agree with the bending moment distribution, allowing for significant weight savings. Fabrication of WT frames might be more expensive, difficult, or even impossible if proper welding technology is not accessible to the fabricator. WT frame manufacturing requires the fabricator ability to realise long welds effectively (i.e. most probably using automated procedure), while controlling the distortion of the members and by minimising the residual stresses induced by the weld.

The direct comparison of the two configurations, the HR frames and the WT frames (Figure 1), is impossible, unless a thorough economic study is carried out. However, even the results of such study are influenced by the economic environment (e.g. labour cost vs. material cost), and the equipment which the fabricator uses. Therefore, the question "*which of the two frame configurations is more economical?*", can only be answered for a particular fabricator operating in a particular market.

Given these complications, it has been opted to concentrate on easily measurable performance parameters, as mass, with the observation that results can easily be expanded to more finance oriented targets. The mass of the frame was selected as an objective for optimization because the PRECASTEEL study is supposed to cover a large geographic area in Europe, and the economic profile in these regions can vary considerably. Also surface area and total length of welds (short and long) are saved together with the frame mass to enable simple adjustment of objective function if needed.

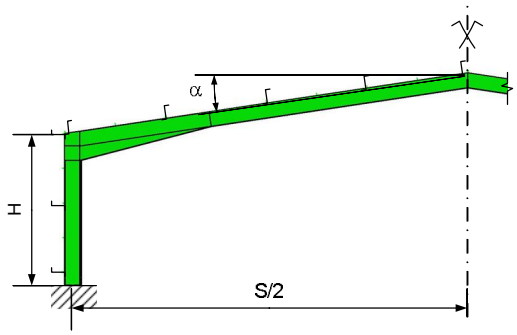

(a-1) Hot-rolled (HR) frames

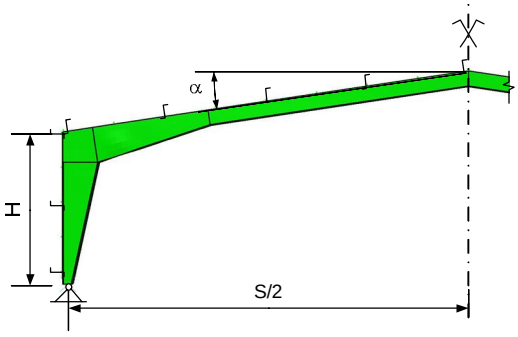

(b-1) Welded tapered (WT) frames

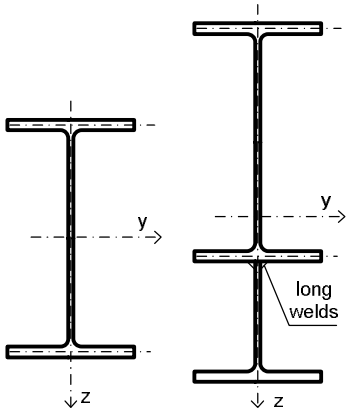

(a-2) Rafter section: constant & haunch

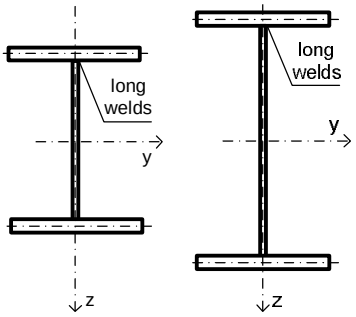

(b-2) Rafter section: constant and tapered

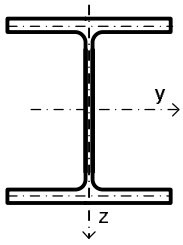

(a-3) Column section

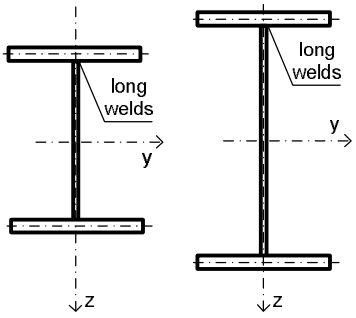

(b-3) Column section: constant and tapered

Figure 1. Geometric configurations of the HR and WT frames.

2 Design methods

Design methods described in the report are divided into three levels according their sophistication, accuracy and time required to perform them. All design methods conform to the Eurocodes [6], and more specifically to EN 1993-1-1 [9]. Scripts were developed under Microsoft Excel and Abaqus in order to carry out automatically the finite element analysis (FEM), and design checks required by the design methods. In the next step, these scripts have been integrated in optimization procedures. The design methods considered are:

Method 1: Global nonlinear analysis (GNLA)
Straightforward numerical calculation by modelling frames with shell type finite element (FE). The calculation is material and geometrically nonlinear, and it takes into account initial imperfections.

Method 2: General method (GMA)
Linear or nonlinear in-plane analysis of the frame, with out-of-plane stability being taken into account by a global reduction factor. Beam model with stepped cross-sections (10 divisions) is used for the in-plane analysis, while shell based model is used for the out-of-plane effects.

Method 3: EC3 interaction formulae (IFM)
Linear in-plane analysis using cross-sectional checks as limit states conditions. Frame modelled using beam type finite elements with stepped cross-sections (4 divisions).

A summary of the modelling techniques used in each method is presented in Table 1.

Table 1. Comparison of modelling techniques used in the three design methods.

	Method 1	Method 2	Method 3
Description	Global non-linear analysis	General method with calculated critical amplifier (EN 1993-1-1)	Interaction of axial compression and bending (EN 1993-1-1)
Software used	**Abaqus**	**Abaqus**	**MS Excel**
Geometry	3D shell model	**2D wire model, 3D shell** for buckling	2D wire model
Tapering	continuous shell	stepped – 10 divisions and continuous shell	stepped – 4 divisions
Global stability	sway imperfections	sway imperfections	sway imperfections
In-plane stability	deformed shape	deformed shape	reduction factors
Out-of-plane stability	deformed shape	global reduction factor	reduction factors
Material plasticity	elastic-plastic mat.	elastic-plastic materia	plastic sect. resistances
Geometric non-linearity	non-linear calculation	non-linear calculation (when needed)	linear calculation with 2nd order amplifier
Calculation steps	**2 steps:** LBA and GMNIA	**3 steps:** LBA-y, LBA-z and GMNIA	**1 step:** LA
Calculation time	**approx. 100 sec.**	**approx. 25 sec.**	**approx. 1 sec.**

The most important difference between three proposed methods is the approach of accounting for out-of-plane stability of the frame.

The GNLA method uses non-linear calculation of the imperfect structure, with imperfections obtained from a linear eigenvalue analysis. Out-of-plane stability is implicitly accounted for by the imperfections, and the nonlinear calculation of the structure.

On the other hand, the method using interaction formulae (IFM) is based on considering buckling by reduction factors for members. Critical loads are calculated for each member separately, based on its slenderness. This approach is not dealing with the whole structure being able to predict the strength of isolated members with ideal (e.g. perfect fixity) support conditions.

The general method (GMA), standing between them in terms of complexity, uses only one reduction factor for out-of-plane buckling, which is related to the overall slenderness of the frame. The method produces more appropriate results than interaction method because stability is calculated using the numerical model of the whole structure, with possibility to consider more realistic support conditions (e.g. partial fixity or eccentric lateral support).

2.1 Global non-linear analysis (GNLA)

Geometrically and Materially Nonlinear Analysis on Imperfect structure (GMNIA) is carried on the shell model. The required initial imperfection is obtained by dislocating the nodes of the mesh with values obtained from an eigen-buckling calculation of the same FE model.

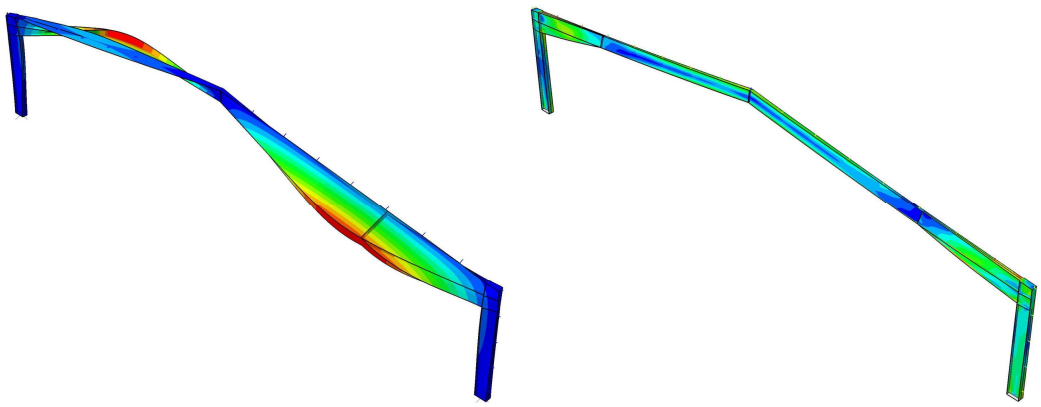

Figure 2. Steps of the Global non-linear analysis.

GNLA starts with an eigenbuckling step in the Abaqus script where three eigenvalues are calculated. The first positive eigenvalue is searched in order to use its buckling shape as source for the initial imperfection. If the first positive eigenvalue does not appear within the first three modes, the script automatically re-submits the analysis with higher number of requested eigenvalues. Node positions (i.e. normalised displacements of nodes in the buckling shape) from the first positive mode are saved and used in the next step.

In the second step of the analysis the loads from accompanying actions are placed on the model, in a static step. Accompanying loads can be:

- The wind load and the crane load, if the analysis is performed to determine the behaviour of the frame in fundamental load combination. In this case it is expected, that the intensity of the accompanying actions is much smaller then that of the leading load (i.e. snow).

- The reduced value of the snow load, which accompanies earthquake loads, if the aim of the analysis is to determine the performance under earthquake loads. In this case snow load is only a small fraction of the design snow load (i.e. 0% or 20% according to EN 1990 [6]), therefore it is expected to be of low intensity.

The third step is a non-linear "Riks" analysis, starting initially with 10% of the total leading load and increasing until the frame collapses. Naturally, the accompanying load also stays on the structure in this step. Initial imperfections are applied corresponding to the first positive buckling shape; they are scaled in amplitude to match EN 1993 [9] bow imperfections. Additional sway imperfections, also conforming to EN 1990 [9], are applied before the second step starts. The sway imperfections correspond to the situation of having initial out-of-verticality of the columns (i.e. columns are straight but inclined). Sway imperfection is applied by adjusting node positions in the Abaqus input file. Following table shows some basic analytical settings:

Table 2. Basic GNLA settings used during the Abaqus modelling.

Object/Method	Parameters	Description
BuckleStep	numEigen=3 (6,9,…) vectors=10 maxIterations=5000	LBA Linear Bifurcation Analysis of the shell model
StaticStep	nlgeom=ON	Pre-loading with accompanying static loads (wind, crane,..)
StaticRiksStep	nlgeom=ON nodeOn=ON initialArcInc=0.1 maxNumInc=500	GMNIA Geometrically and materially non-linear analysis on imperfect structure using shell model loaded with the leading actions

Results are expressed as magnitude of the leading load at which the ultimate limit state (ULS) or serviceability limit state (SLS) is reached. As the leading load is gradually applied to the frame, and because the frame is modelled with non-linearity, therefore pushover type, force vs. displacement, curves can be drawn with the leading load level vs. corresponding displacement. The initial value of displacement is caused by accompanying loads applied in the first step. When the structure collapses in preloading step, the resulting leading load magnitude is zero.

By default, the SLS limits used are S/200 for vertical deflection and H/100 for horizontal deflection. The horizontal limit is derived, in a simplified way, from EN 1998-1: 2004 [10]. Firstly, it is assumed that the frames behave in an elastic way under the design seismic load. Given that seismic design is carried out using a behaviour factor q = 1.5 (see §3.3) this is plausible. Most often, the fundamental load combination is critical for the design and significant elastic overstrength exist in the seismic combination. The second assumption is that the frame can be

modelled as an SDOF oscillator. Therefore, the calculations of Annex B, EN 1998-1:2004 [10] can be used.

If the above two assumptions are accepted then, q_u = 1 (Annex B, [10]); and the displacement behaviour factor is q_d = q, in §4.3.4 of EN1998-1. Therefore, the horizontal displacements at design earthquake level (d_s) can be calculated from displacements obtained from the elastic analysis as:

$$d_s = q_d \cdot d_e \qquad (1)$$

Using the SLS displacement limit, corresponding to ductile non-structural elements being connected to the structure, we have the condition $d_s \cdot \nu \leq 0.0075 \cdot H$, where υ is the reduction factor with the value 0.4 or 0.5 (§4.4.3, EN 1998-1 [10]). Therefore, the elastic displacements have to fulfil the condition:

$$d_s \cdot \nu \leq 0.0075 \cdot H \Rightarrow d_e \leq \frac{0.0075 \cdot H}{q_d \cdot \nu} \approx \frac{0.0075 \cdot H}{1.5 \cdot 0.5} \approx 0.01 \cdot H \qquad (2)$$

One particular case is, when the SLS displacements are not reached even for forces corresponding to the failure of the frame. In this case, the elastic part of the behaviour is extrapolated, and the SLS load is determined for a frame with the same stiffness. This method provides SLS load results in all cases, even when the limit deformation is not physically reached in the analysed model. The existence of an ULS is particularly important during the optimization procedure of the frames (see later), because in this way distinction can be made between frames which all satisfy the SLS criteria, but they have different initial stiffness.

ULS load magnitude is defined where the first yield appears, regardless the plasticity user settings. This is one weakness of the GNLA procedure, where further improvement is needed. However, it was found to be very difficult to extend ULS checking into the plastic range, mainly because a plasticised “cross-section” cannot be recognised in all cases on a shell model. Sometimes plasticity develops in such regions that the plastic cross-section cannot be clearly identified but the rotation of the beam is still possible. E.g. while the tension flange is yielding, the opposite side compression flange is buckling at stress levels less then the yield stress. From the technical point of view this means that a plastic hinge is formed, and the cross-section rotation is happening under a constant bending moment. However, this can be recognised only by visual inspection of the model, or by a sophisticated multi-parameter checking procedure, which proved to be impossible to implement.

Therefore, the calculation using global non-linear analysis is always elastic, and it contains a degree of conservatism depending of the difference between elastic and plastic capacity of the frame. The conservatism is largest for frames made of members with Class 1 cross-sections, it is more moderate for Class 2 cross-section frames, and it disappears for Class 3 frames, where elastic design is required by EN 1993 [9].

2.2 General method analysis (GMA)

According to EN 1993-1-1 [9], overall resistance of a structural component can be verified using following condition:

$$\frac{\chi_{op} \cdot \alpha_{ult,k}}{\gamma_{M1}} \geq 1{,}0 \qquad 3$$

Where: $\alpha_{ult,k}$ - is the minimum load amplifier of the design loads to reach the characteristic resistance of the most critical cross-section without taking out-of-plane buckling into account.

χ_{op} - is the reduction factor to take into account out-of-plane buckling.

γ_{M1} - is the safety factor.

The reduction factor χ_{op} can be calculated using EN 1993 [9] buckling curves, and the global non-dimensional slenderness for out-of-plane buckling, $\overline{\lambda}_{op}$:

$$\overline{\lambda}_{op} = \sqrt{\frac{\alpha_{ult,k}}{\alpha_{cr,op}}} \qquad 4$$

Where $\alpha_{cr,op}$ is the minimum load amplifier of the design loads to reach the elastic critical resistance with regards to lateral or lateral torsional buckling (LTB)

In the GMA, the first step (LBA-z) uses the same shell model and settings as the first step of the GNLA analysis; but instead of storing the perturbed shape, only the critical multiplier $\alpha_{cr,op}$ is retained.

The second and third steps of the GMA is carried out on a wire model of the frame (i.e. members are modelled as beam elements). In the second step the structure is preloaded with accompanying loads in a static step, in a similar procedure as in the GNLA method. In the third static Riks step, the frame is gradually loaded with the leading action until failure. However, before the loading phase starts the geometry is disturbed by initial imperfections resulting from an in-plane buckling analysis of the wire model (LBA-y). These imperfections are taking into account in-plane sway effects [9].

During the Riks step, the failure of the frame is defined differently depending on the cross-section classes of the members. If the frame is made of Class 1 or Class 2 members, failure occurs at full plasticisation of a cross-section (i.e. forming of a plastic hinge). Plastic hinges can now easily be identified by a rapid increase of equivalent plastic strain on the wire model. A limit of the plastic strain equalling 5 times the elastic strain is used in the script. If the frame has Class 3 members, then the first yielding signals the failure of the frame. Alternatively, the user can force the elastic or plastic calculation regardless the section classification. The specific settings of used methods are in following table:

Table 3. Basic GMA settings used during the Abaqus modelling.

Object/Method	Parameters	Description
BuckleStep	numEigen=3 (6,9,…) vectors=10 maxIterations=5000	LBA-y In-plane buckling analysis of wire model LBA-z Out-of-plane buckling analysis of shell model
StaticStep	nlgeom=ON	Preloading with accompanying static loads (wind, crane,..)
StaticRiksStep	nlgeom=ON nodeOn=ON initialArcInc=0.1 maxNumInc=500 minArcInc=0.0000000001	GMNIA Geometrically and materially non-linear analysis on imperfect structure using wire model

Results are also expressed as load levels of the leading load at which the ULS and SLS limit is reached.

2.3 Method using EC3 interaction formulae (IFM)

This method is most commonly used for designing portal frames (and all types of structures). It is based on static calculation of the structure using beam elements in order to determine the internal forces generated by loads. ULS design checks are then carried out on members isolated from the structure (e.g. columns, beams, braces etc.) From the point of view of the member check, the interaction with the rest of the structure is taken into account in a simplified way.

For the buckling check of members subjected to combined axial compression (N) and bending (M), Eurocode 3 [9] provides two alternative methods. They both utilize N-M interaction formulae to account the effects of compression and bending together, and are called Method 1 and Method 2 in Ec3.

Method 2 includes simplified calculation rules of N-M interaction of members, and it is often used by designers for more complex structures. As it is very fast, compared to the GMA and GNLA methods, not requiring numerical calculation of the out-of-plane stability, it has been selected as a third alternative for the design of the frames.

For columns and beams with variable cross-section internal forces are obtained by a static analysis of the structure. The variability of the sections is approximated by using stepwise variation in the FE model. therefore we have:

axial forces N_{Ed},

bending moments to “y” axis $M_{y,Ed}$, (in quarters $M_{y,Ed,1}$ to $M_{y,Ed,5}$)

shear force in “z” direction $V_{z,Ed}$,

assuming that axis “y” is horizontal and the weak direction of bending will be always normal to “z” axis.

cross-sectional resistances (EN 1993-1-1) are calculated as follows:

resistance in compression $N_{Rk} = A \cdot f_y$

resistance in bending to “y” axis $M_{y,Rk} = W_{el,y} \cdot f_y$ for elastic design

resistance in bending to "y" axis $M_{y,Rk} = W_{pl,y} \cdot f_y$ for plastic design

shear resistance in "z" direction $V_{z,Rk} = A_V \cdot f_y / \sqrt{3}$

The calculation is repeated with second order effect amplification factor for slender frames, where the in-plane critical multiplier $\alpha_{cr} \leq 10$ for elastic or $\alpha_{cr} \leq 15$ for plastic analysis.

The second order amplification factor is calculated using Timoshenko formula as:

$$A_f = \frac{1}{1 - \frac{1}{\alpha_{cr}}}$$ and horizontal load $F_{H2,Ed} = A_f F_{H,Ed}$. (EN 1993-1-1, 5.2.2)

The calculation of the critical multiplier (α_{cr}) takes into account the presence of the axial force in the rafters, and utilizes the formulas proposed by Davies [4]:

$$\alpha_{cr} = \frac{5 \cdot E \cdot (10 + R)}{\frac{5 \cdot N_{Ed,b} \cdot s^2}{I_{y,b}} + \frac{2 \cdot R \cdot N_{Ed,c} \cdot h^2}{I_{y,c}}}$$, for fixed base frame (5)

and,

$$\alpha_{cr} = \frac{3 \cdot E \cdot I_{y,b}}{s \cdot (N_{Ed,c} \cdot h + 0{,}3 \cdot N_{Ed,b} \cdot s)}$$, for pinned base frame (6)

Where: E - is the elastic modulus of steel

s, h - are the lengths of beam and column respectively

$N_{Ed,b}, N_{Ed,c}$ - the axial force in the beam and column respectively

$I_{y,b}, I_{y,c}$ - the second moment of area of the beam and column respectively

$R = \frac{I_{y,c} \cdot s}{I_{y,b} \cdot h}$.

Eq. 5 and 6 are developed for constant cross-section frames. In case of variable cross-section members, average values of the second-moments of area are used.

A. Limit states conditions (EN 1993-1-1)

Members subjected to combined bending and axial compression shall satisfy ULS conditions expressed in EC3 as interaction formulae (EN 1993-1-1, 6.3.3):

$$\frac{N_{Ed}}{\chi_y \cdot N_{Rk} / \gamma_{M1}} + k_{yy} \cdot \frac{M_{y,Ed}}{\chi_{LT} \cdot M_{y,Rk} / \gamma_{M1}} \leq 1$$, for FB with LTB effect (7)

And,

$$\frac{N_{Ed}}{\chi_z \cdot N_{Rk}/\gamma_{M1}} + k_{zy} \cdot \frac{M_{y,Ed}}{\chi_{LT} \cdot M_{y,Rk}/\gamma_{M1}} \le 1, \text{ for LTB} \qquad 8$$

Where: $N_{Ed}, M_{y,Ed}$ - are the design value of axial force and major axis bending

$N_{Rk}, M_{y,Rk}$ - are the resistances of the cross-section to axial force and major axis bending

$\chi_Y, \chi_z, \chi_{LT}$ - are reduction factors corresponding to “y” axis FB, “z” axis FB and LTB (See section C of this chapter)

k_{yy}, k_{yy} - are factors taking into account the interaction between axial force and bending moment acting together (See section B of this chapter).

The ULS checks, expressed in eq. 7 and 8, were performed in each cross-section. Even calculation of the class of the cross-section was carried out in each section. This usage of the check is debatable, because eq. 7 and 8 were calibrated for constant cross-section members, and are meant for member check, not cross-section check as used here. However, the interpretation of using them in each cross-section is probably conservative. Additionally, EC3 [9] is not defining design methods for the case of variable members, so some kind of adaptation of the existing methods is inevitable.

The design value of shear force at each cross-section shall also satisfy ULS condition concerning shear resistance:

$$\frac{V_{z,Ed}}{V_{z,Rk}/\gamma_{M0}} \le 1 \qquad 9$$

For serviceability limit state (SLS), as default settings, the maximum of vertical deflection cannot exceed 1/200 of the span, and the horizontal sway 1/300 of its height. However, the used of the software can easily re-define these limits from the input file.

B. N-M interaction factors (k_{yy}, k_{zy})

For elastic calculation of members susceptible to torsion deformations (EN 1993-1-1, Annex B) the following calculation is used:

$$k_{yy} = \min\left[C_{my}\left(1 + 0{,}6 \cdot \bar{\lambda}_y \frac{N_{Ed}}{\frac{\chi_y \cdot N_{Rk}}{\gamma_{M1}}}\right); C_{my}\left(1 + 0{,}6\frac{N_{Ed}}{\frac{\chi_y \cdot N_{Rk}}{\gamma_{M1}}}\right)\right], \text{ and}$$

$$k_{zy} = \max\left[1 - \frac{0{,}05\bar{\lambda}_z}{(C_{mLT} - 0{,}25)}\frac{N_{Ed}}{\frac{\chi_z \cdot N_{Rk}}{\gamma_{M1}}}; 1 - \frac{0{,}05}{(C_{mLT} - 0{,}25)}\frac{N_{Ed}}{\frac{\chi_z \cdot N_{Rk}}{\gamma_{M1}}}\right] \qquad 10$$

Where (besides the previously discussed quantities):

C_{my}, C_{mLT} - are two equivalent moment factors
$\bar{\lambda}_y, \bar{\lambda}_z$ - are non-dimensional slenderness's.

The equivalent uniform moment factors can be calculated with one of the expressions below:

$C_{my} = 0{,}9$ for members with sway buckling mode
$C_{mLT} = \max(0{,}6 + 0{,}4 \cdot \psi\ ; 0{,}4)$, for columns
$C_{mLT} = \max(0{,}2 + 0{,}8 \cdot \alpha_S\ ; 0{,}4)$, for beams where $\alpha_S \geq 0$
$C_{mLT} = \max(0{,}1 - 0{,}8 \cdot \alpha_S\ ; 0{,}4)$, for beams where $\alpha_S < 0$ and $\psi \geq 0$
$C_{mLT} = \max[0{,}1 \cdot (1 - \psi) - 0{,}8 \cdot \alpha_S\ ; 0{,}4]$, for beams where $\alpha_S < 0$ and $\psi < 0$.

With: $\psi = M_{y,Ed,1} / M_{y,Ed,5}$
$\alpha_S = M_{y,Ed,3} / M_{y,Ed,5}$

And, $M_{y,Ed,1}$ to $M_{y,Ed,5}$, are design bending moments in quarter points along the length of the member.

C. Reduction factors due to buckling ($\chi_Y, \chi_z, \chi_{LT}$)

As mentioned earlier, buckling is taken into account by reduction factors depending on the non-dimensional slenderness ($\bar{\lambda}$) of members:

$$\chi = \frac{1}{\phi + \sqrt{\phi^2 - \bar{\lambda}^2}} \qquad 11$$

Where:

$$\phi = 0{,}5 \cdot \left[1 + \alpha \cdot (\bar{\lambda} - 0{,}2) + \bar{\lambda}^2\right]$$

The value of imperfection factors α depend on the buckling curve recommended by Ec3:

$\alpha = 0{,}21$ corresponds to the buckling curve "a",
$\alpha = 0{,}34$ corresponds to the buckling curve "b",
$\alpha = 0{,}49$ corresponds to the buckling curve "c",
$\alpha = 0{,}76$ corresponds to the buckling curve "d".

The non-dimensional slenderness for FB, TB and TFB is calculated as:

$$\bar{\lambda} = \sqrt{\frac{N_{Rk}}{N_{cr}}}, \text{ where } N_{cr} = \min\left(N_{cr,FBy}, N_{cr,FBz}, N_{cr,TB}, N_{cr,TFB}\right) \qquad 12$$

Where: N_{Rk} - is the characteristic resistance of the cross-section
N_{cr} - is the minimum of member elastic critical loads.

The application of eq. 12 is also controversial, because of the variability of the cross-section along the member. In the calculation of the critical force in the "y" (major axis) direction, the tapering/variation was taken into account using the method proposed by Šapalas [2]. Minor axis buckling is not significantly influenced by the variation of the cross-section, because the minor axis second moment of area does not vary significantly due to the increase of height of the profile. According to Šapalas [2], the major axis ("y") critical force $N_{cr,FBy}$ of the variable member is calculated by reducing the critical force determined with the maximum cross-section properties.

The critical loads corresponding to flexural buckling modes are calculated as:

$$N_{cr,FBz} = \frac{\pi^2 \cdot E \cdot I_{z,\min}}{a^2}, \text{ minor axis FB between two lateral supports}$$

$$N_{cr,FBy} = \alpha_n \frac{\pi^2 \cdot E \cdot I_{y,\max}}{L_{cr,y}^2}, \text{ major axis FB for tapered member} \qquad 13$$

$$N_{cr,FBy} = \left(I_{y,\max} \frac{L_h}{S/2} \alpha_n + I_{y,\min} \frac{S/2 - L_h}{S/2} \right) \frac{\pi^2 \cdot E}{L_{cr,y}^2}, \text{ major axis FB for member with haunch}$$

Where: $I_{z,\min}$ - weak axis second moment of area at the small member section
a - distance between lateral supports
$I_{y,\max}$ - strong axis second moment of area at large member section
$L_{cr,y}$ - critical length for strong axis FB
α_n - reduction factor proposed by Šapalas [2]
S - the span of the frame.

For torsional (TB) and torsional flexural buckling (TFB), the critical loads are calculated using the following expressions:

$$N_{cr,TB} = \frac{\left(I_{w,\min} \cdot E \cdot \pi^2 / a^2\right) + G \cdot I_{t,\min}}{i_0^2} \text{ (between two lateral supports)}$$

$$N_{cr,TFB} = \frac{\left(I_{w,\min} + I_{z,\min} \cdot e_z^2\right) \cdot \left(E \cdot \pi^2 / L^2\right) + G \cdot I_{t,\min}}{e_{z,\min}^2 + i_0^2} \text{ (whole member)} \qquad 14$$

Where: $I_{w,\min}$ - is the warping constant of the shallow cross-section
$I_{t,\min}$ - torsional constant of the shallow cross-section
G - shear modulus
i_0 - polar radius of gyration
e_z - the eccentricity of lateral supports in the weak axis direction, from the shear centre of the CS. E.g. purlins connected to the upper flange of the beam provide an eccentric lateral support in the weak direction. If the purlins are fixed to the upper flange, then e_z is equal to half the height of the beam.

The $N_{cr,TFB}$ expression, adapted from Timoshenko [1] was developed for members with continuous lateral supports. In case of lateral support in points, the presumption is that supports are placed at small enough intervals, so as to act similarly as if they were continuous. This condition is met by the most common purlin distributions (e.g. 1200-2000 mm purlin intervals). FEM studies performed in this project, but also by Aswandy [13] showed that, once there are enough lateral supports to force TFB in a member, the critical load is not significantly increased by providing more supports. Certainly, $N_{cr,TFB}$ is slightly overestimated by using Eq 14. On the other hand, the torsional support provided by the purlins is completely neglected, which is conservative.

The non-dimensional slenderness for lateral torsional buckling (LTB) is calculated as:

$$\bar{\lambda}_{LT} = \sqrt{\frac{M_{y,Rk}}{M_{cr}}} \qquad 15$$

Where: $M_{y,Rk}$ - is the major axis bending resistance (elastic or plastic depending on design method); while the formulae for critical moment (M_{cr}) was considered according to Šapalas [2] and prENV 1993-1-1, Annex F:

Critical moment used in calculation is smaller value of critical moment of restrained member between fork supports according to SCI Technical Report [15] and critical moment of unrestrained part of member between purlins according to Eurocode 3.

$$M_{cr} = \min\left[\left(\frac{1}{m_t c^2}\right)M_{cr0}, \quad C_1\frac{\pi^2 E\cdot I_{z,\min}}{a^2}\sqrt{\frac{I_{w,\min}}{I_{z,\min}}+\frac{a^2 G\cdot I_{t,\min}}{\pi^2 E\cdot I_{z,\min}}}\right], \qquad 16$$

$$M_{cr0} = \left(\frac{i_0^2}{2e_z}\right)N_{cr,TFB} \qquad 17$$

Where $I_{z,\min}, I_{t,\min}, I_{w,\min}$ are sectional properties of the shallow end,
a is the distance between lateral supports (purlins, side rails)
$N_{cr,TFB}$ is critical axial load for torsional flexural buckling
C_1 is the moment gradient factor from Eurocode 3
e_z is the distance from shear centre to lateral support either at shallow end or at deep end of tapered beam

If $\bar{\lambda}_{LT} > 1{,}0$, equivalent section factor is taken as 1,0 and the minimum M_{cr0} is used, which come from the deepest end ($e_{z,\max}$ is used also for calculation of $N_{cr,TFB}$). In all other cases we use $e_{z,\min}$ and following expression for equivalent section factor:

$c = c_0$ for tapered members and

$c = 1 + (c_0 - 1)\sqrt{L_h / L}$ for members with haunches 18

Equivalent uniform moment factor [15] for tapered member without loads between lateral-torsional restraints is:

$$m_t = \frac{1}{12}\left(\frac{M_{c,Rd}}{M_{Sd}}\right)_{\min}\left(\frac{M_{Sd1}}{M_{c,Rd1}} + \frac{3M_{Sd2}}{M_{c,Rd2}} + \frac{4M_{Sd3}}{M_{c,Rd3}} + \frac{3M_{Sd4}}{M_{c,Rd4}} + \frac{M_{Sd5}}{M_{c,Rd5}} + 2\mu_{SE}\right), \quad 19$$

where only positive values of M_{Sd} and μ_{SE} are included.

$M_{Sd1}...M_{Sd5}$ are design bending moments at quarter spans,
$M_{c,Rd1}...M_{c,Rd5}$ are design bending resistances at quarter spans,

$$\left(\frac{M_{c,Rd}}{M_{Sd}}\right)_{\min} = \min\left(\frac{M_{c,Rd1}}{M_{Sd1}}, \ldots, \frac{M_{c,Rd5}}{M_{Sd5}}\right) \quad 20$$

$$\mu_{SE} = \max\left(\frac{M_{c,Rd2}}{M_{Sd2}}, \frac{M_{c,Rd3}}{M_{Sd3}}, \frac{M_{c,Rd4}}{M_{Sd4}}\right) - \max\left(\frac{M_{c,Rd1}}{M_{Sd2}}, \frac{M_{c,Rd5}}{M_{Sd5}}\right) \quad 21$$

An alternative calculation of relative slenderness [15] is also used in the script

$$\overline{\lambda}_{LT} = c\sqrt{m_t}\sqrt{\frac{W_{y,\max}}{A_{\max}} \cdot \frac{2e_z}{i_0^2}}\lambda, \quad 22$$

Where $\lambda = \dfrac{L/i_z}{\sqrt{\alpha + \dfrac{I_{t,\max}L^2}{2{,}6\pi^2 I_{z,\max} i_0^2}}}$ and $\alpha = \dfrac{e_z^2 + I_{w,\max}/I_{z,\max}}{i_0^2}$ 23

3 Loading scenarios

According to the load settings, the script automatically selects if vertical or horizontal loads are to be increased gradually. If snow is the leading load, then the structure is preloaded with other accompanying loads (e.g. wind, crane load), and the snow load is gradually increased until failure. If e.g. earthquake is the leading load, then the structure is preloaded with snow, and the earthquake load is increased until failure.

In the fundamental load combination, snow load is considered to be the leading variable action and a combination of actions for persistent or transient design situation is calculated as follows:

$$\gamma_{G,\mathrm{sup}} G_k + \gamma_S S_k + \gamma_W \psi_{0,W} W_k + \gamma_C \psi_{0,C} C_k \quad \text{(EN 1990 6.10)} \qquad 24$$

Where: G_k is the characteristic dead load ($\gamma_{G,\mathrm{sup}} = 1.35$)

S_k is the characteristic snow load ($\gamma_S = 1.5$)

W_k is the characteristic wind load ($\gamma_W = 1.5, \psi_{0,W} = 0.6$)

C_k is the characteristic crane load ($\gamma_C = 1.5, \psi_{0,C} = 1.0$).

For the horizontal pushover analysis with constant vertical load the seismic design situation applies:

$$G_k + A_{Ed} + \psi_{2,S} S_k + \psi_{2,C} C_k \quad \text{(EN 1990 6.12)} \qquad 25$$

Where: A_{Ed} is the design seismic load

and the combination factors are $\psi_{2,W} = 0.0, \psi_{2,S} = 0.2, \psi_{2,C} = 0.8$

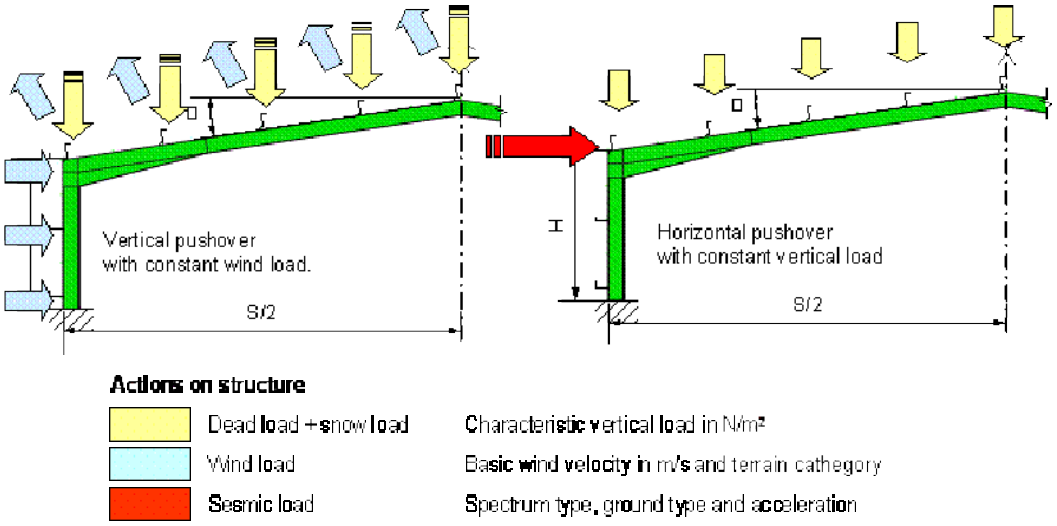

Figure 3. Loading scenarios.

3.1 Dead load and snow load

The design value of vertical snow and dead loads can be inserted in the input file in kN/m^2 (as distributed load). In case of dead load the value should also contain the estimation of the self-weight of the frame, including purlins and side-rails. This is necessary because as the mass of the frame is not transformed into weight in the model (i.e. gravity is 0).

3.2 Wind load

Calculation of wind actions follows EN 1991-1-4 [7]. The script uses simplified calculation of external wind pressure based on the exposure factor. The wind load spanning different zones is averaged and each face is loaded with constant pressure.

The basic calculation of external wind pressure is $w_e = q_p(z) \cdot c_{pe}$, or, expressed using the exposure factor:

$$w_e = q_b \cdot c_e(z) \cdot c_{pe} \qquad 26$$

Where: w_e is the wind pressure acting on the external surfaces
z is the reference height for external pressure (§6.3, [7])
$c_e(z)$ is the exposure factor given §4.5 of EN 1991-1-4 [7]
c_{pe} is the pressure coefficient for external pressure.

Since the exposure factor is the ratio of peak velocity pressure and basic velocity pressure:

$$c_e(z) = \frac{q_p(z)}{q_b} \qquad 27$$

We can write:

$$c_e(z) = \frac{\left[1 + 7 \cdot I_v(z)\right]\frac{1}{2} \cdot \rho \cdot v_m^2(z)}{\frac{1}{2} \cdot \rho \cdot v_b^2} = c_r^2(z) \cdot c_0^2(z) \cdot \left[1 + 7 \cdot I_v(z)\right] = \qquad 28$$

$$= c_r^2(z) \cdot c_0^2(z) \cdot \left[1 + 7 \cdot \frac{k_l}{c_0(z) \cdot \ln(z / z_0)}\right]$$

Where: $c_r(z)$ is the roughness factor
$c_0(z)$ is the orography factor
k_l Is the turbulence factor
z_0 is the roughness length.

The turbulence factor k_l and orography factor c_0 are considered to be 1.0, according to §4.3.1 and §4.4.(1) of EN 1991-1-4 [7]. Hence the exposure factor expression can be reduced to the more simple form used in the Python script:

$$c_e(z) = c_r^2(z) \cdot \left[1 + \frac{7}{\ln(z/z_0)}\right] = c_r^2(z) + 7 \cdot k_r \cdot c_r(z) \quad (29)$$

Where: k_r is a terrain factor depending on the roughness length z_0 from §4.3.2 [7].

In the script, the terrain factor k_r and roughness factor $c_r(z)$ are calculated according §4.3.2 of EN 1991-1-4 [7]. The ridge of the frame is used for defining the reference height of wind load calculation (z).

3.3 Seismic load

The seismic design loads are calculated out according to EN1998-1:2004 [10]. The masses, from vertical loads from Eq. 25 acting on the frame during earthquake, are concentrated in a single point at roof level (M_{eq}). I.e. the frame is transformed in a single degree of freedom (SDOF) oscillator.

The lateral stiffness of the frame is pre-calculated by applying two unit concentrated forces in the corners of the frame (F_1 = 1 kN). From these loads, the horizontal deflection (Δ_1) of the frame corner is calculated, and the lateral stiffness is evaluated as $K_{lat} = 2 \cdot F_1/\Delta_1$. The earthquake mass and the lateral stiffness are used to evaluate the fundamental period of vibration of the frame:

$$T = 2 \cdot \pi \cdot \sqrt{\frac{M_{eq}}{K_{lat}}} \quad (30)$$

Earthquake action is calculated using the lateral force method of analysis (§4.3.3.2 from [10]). It is checked that $T < \min(4 \cdot T_c, 2s)$, so that he validity of the method is ensured. The seismic base shear force F_b is calculated as:

$$F_b = S_d(T) \cdot M_{eq} \cdot \lambda \quad (31)$$

Where: $S_d(T)$ is the ordinate of the design spectrum
M_{eq} is the earthquake mass
λ is a correction factor for multi-storey buildings (λ = 1 is used in the script).

The design spectrum is calculated according to EN 1998-1 [10] as:

$$S_d(T) = \begin{cases} a_g \cdot S \cdot \left[\frac{2}{3} + \frac{T}{T_B} \cdot \left(\frac{2.5}{q} - \frac{2}{3} \right) \right], \text{for } 0 \le T \le T_B \\ a_g \cdot S \cdot \frac{2.5}{q}, \text{for } T_B \le T \le T_C \\ \max\left(a_g \cdot S \cdot \frac{2.5}{q} \cdot \frac{T_C}{T}, \beta \cdot a_g \right), \text{for } T_C \le T \le T_D \\ \max\left(a_g \cdot S \cdot \frac{2.5}{q} \cdot \frac{T_C \cdot T_D}{T^2}, \beta \cdot a_g \right), \text{for } T_D \le T \end{cases} \quad (32)$$

Where: a_g is the design ground acceleration on Type A ground
S is the soil factor
T_B, T_C, T_D are the corner/control periods defining the shape of the spectra
q is the behaviour factor.

While a_g is an input which should be defined directly in the "*input.txt*" file, S and the corner periods T_B, T_C, T_D are a function of the spectrum type (i.e. Type 1 or Type 2)and the type of the ground (i.e. A, B, C, D, E, F). The spectrum type and the ground type can be defined in the input file of the analysis.

An all analysis the value of q = 1,5 is adopted for the behaviour factor. This value can not be modified by the user from "*input.txt*".

The calculated base shear force F_b, is divided into two equal concentrated forces acting on the corners of the single span frame.

3.4 Crane load

The crane load is calculated according to EN 1991-3 [8]. User specifies only payload of the crane in the input file. The rest of crane parameters are automatically selected from crane specification file *"cranes.txt"*.

Self-weight Q_C of the crane without lifting attachment is approximately:

$$Q_c \approx 4Q_{r,\min} \quad (33)$$

Hoist load Q_H includes the masses of the payload, the lifting attachment and a portion of the suspended hoist ropes or chains moved by the crane structure:

$$Q_H \approx 2Q_{r,\max} + 2Q_{r,\min} - Q_C \quad (34)$$

Drive force calculation assumes steel-to-steel contact:

$$K = \mu \sum Q_{r,\min} = 0{,}2 \cdot 2 \cdot Q_{r,\min} \quad (35)$$

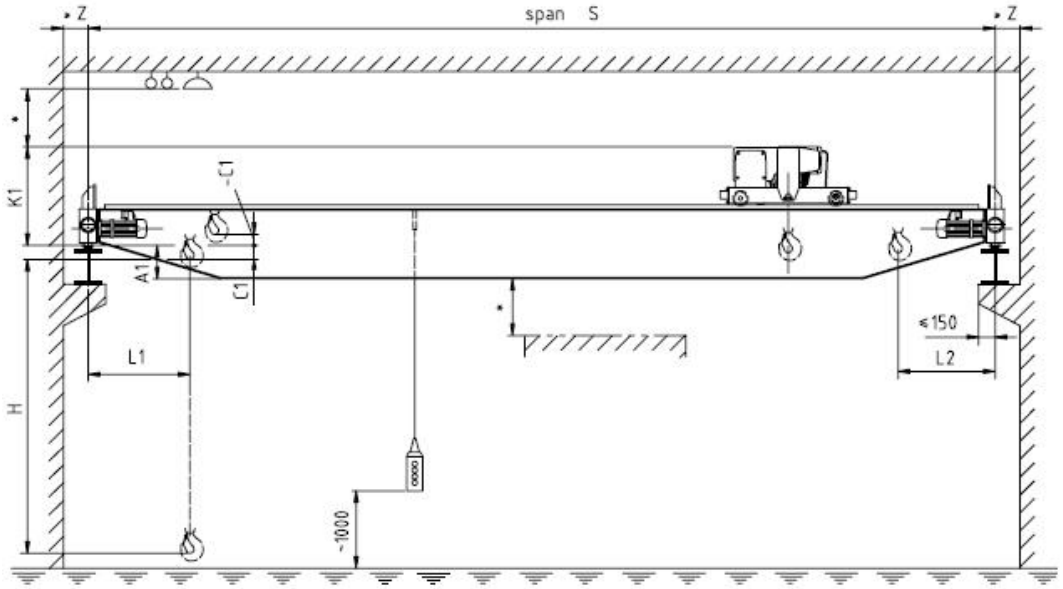

Figure 4. Safety distances used in crane specification file.

Transverse loads are calculated as:

$$H_T = \max(\xi_1, \xi_2)\frac{M}{a} = \max(\xi_1, \xi_2)\frac{Kl_S}{a} = \max(\xi_1, \xi_2)\frac{K(\xi_1 - 0{,}5)l}{a},$$

where $\xi_1 = \dfrac{Q_{r,\max}}{Q_{r,\max} + Q_{r,\min}}$ and $\xi_2 = 1 - \xi_1$.

Skew loads are calculated as:

$$H_S = \lambda_S f \cdot Q_{r,\max} = \max(\xi_1, \xi_2)\left(1 - \frac{a}{2L_k}\right) f \cdot Q_{r,\max},$$

where $f = 0{,}3$.

Design vertical and horizontal load is calculated using following simplified equations:

$P_{vert,\max} = \varphi_1 Q_C + \varphi_2 Q_H$ maximum vertical load,

$P_{vert,\min} = \varphi_1 Q_C$ minimum vertical load,

$P_{hor} = \max(\varphi_5 H_T; H_S)$ horizontal load,

where dynamic factors are $\varphi_1 = 1{,}1$, $\varphi_2 = 1{,}99$, $\varphi_5 = 1{,}5$.

4 Calculation results

Within the cooperation with University of Thessaly on the PRECASTEEL project, we used the analytical tools for verification of the previously published preliminary designs [11].

In the preliminary calculations, purlins were placed at 2000 mm intervals, and frame girders and columns were assumed to have “fork” supports at every second purlin. This means that, the frame had a laterally and a torsion support every second purlin (i.e. at 4000 mm intervals). The assumption concerning torsional support is not usually guarantied by common detailing; i.e. unless special detailing is adopted to physically support the lower flange of the beams and columns. Because a large difference of bending stiffness between the beams and the purlins, it is also not sure that flexible purlins can provide effective torsion support to the frame elements.

Therefore, in the calculations we completely neglected the inner flange lateral supports, and considered the purlins to support the frames only at the top flange level where the purlins main support connection is located.

4.1 Re-calculation of the PRECASTEEL frames

Design situations (EN 1990):
Persistent and transient design situation with dead, snow and reduced wind load
Seismic design situations with seismic, dead and reduced snow load

We calculated two basic load combination types. For the persistent and transient design situation (fundamental load combination) we used the snow load as leading variable action. The frame is pre-loaded with accompanying loads (e.g. wind, imperfections etc.) and the vertical load is gradually increased until failure of the frame:

$$\gamma_{G,\mathrm{sup}} G_k + \gamma_S S_k + \gamma_W \psi_{0,W} W_k + \gamma_C \psi_{0,C} C_k \quad \text{(EN 1990 6.10)} \qquad 36$$

Where: G_k is the characteristic dead load ($\gamma_{G,\mathrm{sup}} = 1.35$)
S_k is the characteristic snow load ($\gamma_S = 1.5$)
W_k is the characteristic wind load ($\gamma_W = 1.5, \psi_{0,W} = 0.6$)
C_k is the characteristic crane load ($\gamma_C = 1.5, \psi_{0,C} = 1.0$).

For seismic design, a horizontal pushover analysis with constant vertical load was carried out. In this case, horizontal loads are gradually increased until failure of the frame.

$$G_k + A_{Ed} + \psi_{2,S} S_k + \psi_{2,C} C_k \quad \text{(EN 1990 6.12), where} \qquad 37$$

Where: A_{Ed} is the design seismic load,
and the combination factors are $\psi_{2,W} = 0.0, \psi_{2,S} = 0.2, \psi_{2,C} = 0.8$.

Design methods:
*General method**:** Linear or nonlinear in-plane analysis using beam model with stepped cross-section, with global reduction for out-of-plane stability. Out of plane stability separately calculated using shell based model of the frame.*
Global non-linear analysis: Geometrical and material non-linear analysis including initial imperfections; the method was used for verification of selected failing frames previously calculated with the General method

The out-of-plane stability can be the most critical failure mode also in hot-rolled frames. Therefore, the design methods we selected take into account, in a quite sophisticated way using shell FEM's, the out-of-plane buckling of frames.

Constants:
Distance between frames: 6 m
Haunch length: 9.1% (1/11) of span, 18.2% (1/5.5) of frame half
Roof angle: 15.0 % (8.53°)
Dead load: 380 N/m^2
Wind load: 30 m/s, terrain type 2 (only in fundamental load combinations)
Seismic load: spectrum type 1, ground type B, q = 1.5
Material: S275

Variable parameters:
Span: 16 m, 20 m, 24 m, 27 m, 30 m, 32 m
Height: 6 m, 8 m
Snow load: 750 N/m^2, 1500 N/m^2
Peak ground acceleration (PGA): 0.32 g, 0.16 g, 0.08 g
Base support: Fixed, Pinned

Considering all variable parameters (including the persistent/transient design situation with no seismic load) makes 192 possible configurations that can be calculated with our tools. We analyzed all cases from Table 4; these frames were pre-designed by University of Thessaly [11].

Table 4. Frame configurations selected for recalculation.

Case	Span	Height	Base Fixed (F) Pinned (H)	Snow load (kN/m^2)	Peak ground acceleration	Column	Rafter
1.1	16 m	6 m	F	0.75	0.32 g	HEA 280	IPE 330
1.2	20 m	6 m	F	0.75	0.32 g	HEA 300	IPE 360
1.3	24 m	6 m	F	0.75	0.32 g	HEA 340	IPE 450
1.4	27 m	6 m	F	0.75	0.32 g	HEA 400	IPE 450
1.5	30 m	6 m	F	0.75	0.32 g	HEA 450	IPE 500
1.6	32 m	6 m	F	0.75	0.32 g	HEA 500	IPE 550
1.8	20 m	8 m	F	0.75	0.32 g	HEA 320	IPE 400
1.16	16 m	6 m	F	1.5	0.32 g	HEA 340	IPE 360
1.17	20 m	6 m	F	1.5	0.32 g	HEA 400	IPE 400
1.18	24 m	6 m	F	1.5	0.32 g	HEA 500	IPE 500
1.19	27 m	6 m	F	1.5	0.32 g	HEA 550	IPE 550
1.20	30 m	6 m	F	1.5	0.32 g	HEA 650	IPE 600
1.21	32 m	6 m	F	1.5	0.32 g	HEA 650	IPE 600
1.23	20 m	8 m	F	1.5	0.32 g	HEA 400	IPE 450
1.31	16 m	6 m	H	1.5	0.32 g	HEA 340	IPE 400
1.32	20 m	6 m	H	1.5	0.32 g	HEA 450	IPE 450
2.1	16 m	6 m	F	0.75	0.16 g	HEA 280	IPE 300
2.2	20 m	6 m	F	0.75	0.16 g	HEA 300	IPE 330
2.3	24 m	6 m	F	0.75	0.16 g	HEA 360	IPE 400
2.4	27 m	6 m	F	0.75	0.16 g	HEA 400	IPE 450
2.5	30 m	6 m	F	0.75	0.16 g	HEA 450	IPE 500
2.6	32 m	6 m	F	0.75	0.16 g	HEA 450	IPE 500
2.8	20 m	8 m	F	0.75	0.16 g	HEA 320	IPE 330
2.20	16 m	6 m	F	1.5	0.16 g	HEA 340	IPE 360
2.21	20 m	6 m	F	1.5	0.16 g	HEA 400	IPE 400
2.22	24 m	6 m	F	1.5	0.16 g	HEA 500	IPE 500
2.23	27 m	6 m	F	1.5	0.16 g	HEA 550	IPE 550
2.24	30 m	6 m	F	1.5	0.16 g	HEA 650	IPE 600
2.25	32 m	6 m	F	1.5	0.16 g	HEA 650	IPE 600
2.27	20 m	8 m	F	1.5	0.16 g	HEA 400	IPE 400
3.1	16 m	6 m	F	1.5	0.08 g	HEA 340	IPE 360
3.2	20 m	6 m	F	1.5	0.08 g	HEA 400	IPE 400
3.3	24 m	6 m	F	1.5	0.08 g	HEA 500	IPE 500
3.4	27 m	6 m	F	1.5	0.08 g	HEA 550	IPE 550
3.5	30 m	6 m	F	1.5	0.08 g	HEA 650	IPE 600
3.6	32 m	6 m	F	1.5	0.08 g	HEA 650	IPE 600
3.8	20 m	8 m	F	1.5	0.08 g	HEA 400	IPE 400
3.20	16 m	6 m	H	1.5	0.08 g	HEA 340	IPE 360
3.21	20 m	6 m	H	1.5	0.08 g	HEA 450	IPE 400
3.22	24 m	6 m	H	1.5	0.08 g	HEA 550	IPE 500
3.23	27 m	6 m	H	1.5	0.08 g	HEA 600	IPE 600
3.24	30 m	6 m	H	1.5	0.08 g	HEA 650	IPE 600
3.25	32 m	6 m	H	1.5	0.08 g	HEA 700	IPE 600

Configurations from Table 4 were recalculated using the general method, both for the fundamental load combinations and for the seismic load combination.

For the fundamental load combination, the vertical loads (i.e. dead & snow) were gradually increased, and results are expressed as limit loads in N/m^2. Before the application of the vertical loads, frames were preloaded with all horizontal actions, including imperfections. In seismic design situation horizontal pushover force was applied, while vertical preload was constant. In this case, results are expressed in kN. In Table 5 we present the limit loads (elastic resistance, plastic resistance, SLS resistance) compared to design and characteristic loads.

Table 5. Limit loads vs. design and characteristic loads for the selected frames.

Evaluation of selected cases

Minimum percentage of exceeding the SLS and ULS limits is calculated.

Case	Profiles	Design load	Elastic resistance	Plastic resistance	Characteristic load	SLS resistance	comment
	Column Beam	kN (horiz.) N/m^2 (vert.)	kN N/m^2	kN N/m^2	kN N/m^2	kN N/m^2	
1.1	HE280A IPE330	33.08 1638.00	117.60 2140.00	156.00 2526.00	33.08 1130.00	74.19 1834.00	54% conservative
1.2	HE300A IPE360	41.26 1638.00	130.40 1745.00	173.80 2019.00	41.26 1130.00	94.08 1522.00	23% conservative
1.3	HE340A IPE450	49.48 1638.00	160.60 1612.00	205.90 1850.00	49.48 1130.00	154.7 1905.00	13% conservative
1.4	HE400A IPE450	55.7 1638.00	174.20 1570.00	210.10 1732.00	55.7 1130.00	195.3 1804.00	6% conservative
1.5	HE450A IPE500	61.9 1638.00	203.60 1611.00	240.40 1761.00	61.9 1130.00	270.9 2143.00	8% conservative
1.6	HE500A IPE550	66.07 1638.00	241.80 1753.00	280.70 1905.00	66.07 1130.00	349.7 2610.00	16% conservative
1.8	HE320A IPE400	41.3 1638.00	131.60 1937.00	173.90 2333.00	41.3 1130.00	77.95 1619.00	42% conservative
1.16	HE340A IPE360	42.59 2763.00	187.30 3071.00	239.30 3928.00	42.59 1880.00	126.3 2999.00	42% conservative
1.17	HE400A IPE400	53.19 2763.00	221.50 2487.00	277.80 3139.00	53.19 1880.00	183.9 2661.00	14% conservative
1.18	HE500A IPE500	63.88 2763.00	289.60 2686.00	346.50 3270.00	63.88 1880.00	356 3778.00	18% conservative
1.19	HE550A IPE550	71.84 2763.00	318.10 2616.00	375.40 3098.00	71.84 1880.00	433.3 3950.00	12% conservative
1.20	HE650A IPE600	79.93 2763.00	377.90 2691.00	434.50 3163.00	79.93 1880.00	624.4 4564.00	14% conservative
1.21	HE650A IPE600	85.16 2763.00	349.90 2361.00	400.00 2737.00	85.16 1880.00	610.1 3996.00	-1% vertical capacity
1.23	HE400A IPE450	53.19 2763.00	187.30 2811.00	238.20 3274.00	53.19 1880.00	137.4 2769.00	18% conservative
1.31	HE340A IPE400	36.4 2763.00	107.9 3147.00	135 3669.00	36.4 1880.00	35.77 2608.00	-2% horizontal deflection
1.32	HE450A IPE450	50.14 2763.00	126.7 2560.00	160.4 3201.00	50.14 1880.00	51.21 2889.00	2% conservative
2.1	HE280A IPE300	16.54 1638.00	91.60 1804.00	108.60 2355.00	16.54 1130.00	64.8 1491.00	32% conservative

Case	Profiles	Design load	Elastic	Plastic	Char.load	SLS resistance	Comment	
		kN, N/m^2	kN, N/m^2	kN, N/m^2	kN, N/m^2	kN, N/m^2		
2.2	HE300A	20.63	91.39	104.20	20.63	80.45	8%	conservative
	IPE330	1638.00	1489.00	1847.00	1130.00	1225.00		
2.3	HE360A	24.76	120.60	132.40	24.76	144	21%	conservative
	IPE400	1638.00	1702.00	1976.00	1130.00	1598.00		
2.4	HE400A	27.85	118.30	129.50	27.85	195.3	6%	conservative
	IPE450	1638.00	1570.00	1732.00	1130.00	1804.00		
2.5	HE450A	30.95	132.90	143.80	30.95	270.9	8%	conservative
	IPE500	1638.00	1611.00	1761.00	1130.00	2143.00		
2.6	HE450A	32.98	120.00	129.40	32.98	265	-7%	vertical capacity
	IPE500	1638.00	1398.00	**1521.00**	1130.00	1891.00		
2.8	HE320A	20.65	87.27	98.96	20.65	56.19	-4%	vertical deflection
	IPE330	1638.00	1553.00	1871.00	1130.00	**1089.00**		
2.20	HE340A	21.29	163.20	194.50	21.29	126.3	42%	conservative
	IPE360	2763.00	3071.00	3928.00	1880.00	2999.00		
2.21	HE400A	26.59	171.00	191.10	26.59	184	14%	conservative
	IPE400	2763.00	2487.00	3139.00	1880.00	2661.00		
2.22	HE500A	31.94	201.90	220.70	31.94	356.2	18%	conservative
	IPE500	2763.00	2686.00	3270.00	1880.00	3778.00		
2.23	HE550A	35.92	212.10	229.50	35.92	434.5	12%	conservative
	IPE550	2763.00	2616.00	3098.00	1880.00	3950.00		
2.24	HE650A	39.96	240.80	257.10	39.96	624.4	14%	conservative
	IPE600	2763.00	2691.00	3163.00	1880.00	4564.00		
2.25	HE650A	42.58	218.60	232.70	42.58	610.1	-1%	vertical capacity
	IPE600	2763.00	2361.00	2737.00	1880.00	3996.00		
2.27	HE400A	26.59	148.10	169.90	26.59	112	8%	conservative
	IPE400	2763.00	2319.00	2976.00	1880.00	2135.00		
3.1	HE340A	10.64	115.20	123.80	10.64	126.4	42%	conservative
	IPE360	2763.00	3071.00	3928.00	1880.00	2999.00		
3.2	HE400A	13.29	103.70	108.10	13.29	184	14%	conservative
	IPE400	2763.00	2487.00	3139.00	1880.00	2661.00		
3.3	HE500A	15.97	118.5	123.7	15.97	356.2	18%	conservative
	IPE500	2763.00	2686.00	3270.00	1880.00	3778.00		
3.4	HE550A	17.96	121.5	126.3	17.96	434.7	12%	conservative
	IPE550	2763.00	2616.00	3098.00	1880.00	3950.00		
3.5	HE650A	19.98	135	139.6	19.98	624.4	14%	conservative
	IPE600	2763.00	2691.00	3163.00	1880.00	4564.00		
3.6	HE650A	21.29	121.4	125.5	21.29	610.1	-1%	vertical capacity
	IPE600	2763.00	2361.00	2737.00	1880.00	3996.00		
3.8	HE400A	13.29	95.92	100.90	13.29	112	8%	conservative
	IPE400	2763.00	2319.00	2976.00	1880.00	2135.00		
3.20	HE340A	8.124	65.09	76.34	8.124	28.23	28%	conservative
	IPE360	2763.00	3181.00	3689.00	1880.00	2397.00		
3.21	HE450A	10.71	67.71	76.52	10.71	36.73	4%	conservative
	IPE400	2763.00	2361.00	2867.00	1880.00	2354.00		
3.22	HE550A	15.88	96.33	105.90	15.88	67.88	0%	
	IPE500	2763.00	2245.00	2765.00	1880.00	2803.00		
3.23	HE600A	17.99	134.50	143.30	17.99	112.4	21%	conservative
	IPE600	2763.00	2925.00	3341.00	1880.00	3921.00		
3.24	HE650A	19.98	114.60	121.30	19.98	106.4	-1%	vertical capacity
	IPE600	2763.00	2277.00	2724.00	1880.00	3240.00		
3.25	HE700A	21.32	104.90	110.70	21.32	100.9	-11%	vertical capacity
	IPE600	2763.00	2113.00	**2450.00**	1880.00	2991.00		

As shown by the differences between the resistances and the design loads (Table 5), the method used for the preliminary design produced conservative results. As it can be observed, the design of almost all these frame configurations is governed by the ULS check in the fundamental load combination. The results of the ULS and SLS checks, in the fundamental load combination are presented in Figure 5, as a function of the span. It can be observed that, while for shorter spans the pre-design procedure produced very safe frames (ULS safety factor of up to 50%), as span increases the safety is diminished. At 32m span frames, some configurations are not safe. This tendency shows how the slenderness of the frames for larges spans is not properly accounted by the beam model based pre-design procedure.

Small (i.e. 4%) SLS failure from the fundamental combination was only encountered for one 20m frame (Figure 5).

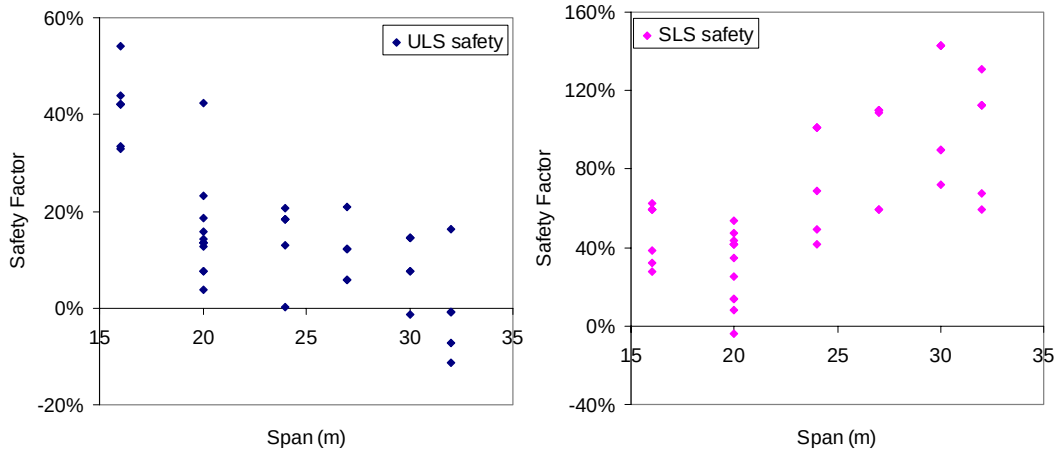

Figure 5. ULS safety factor and SLS safety factor from fundamental loads.

Earthquake loads have not caused ULS check failures in any of these frames. In fact ULS safety factors from the earthquake load combination range from 220% to 1064%. In other words, even with a very large earthquake load (PGA = 0.32g), these frames do not fail the ULS check. SLS check from the earthquake load combination has failed by 2% in case of hinged base frames with 150kg/m^2 snow load and very large earthquake.

In conclusion, we can affirm that the pre-design procedure used by the University of Thessaly [11] was: (1) generally safe, but (2) too conservative for small span frames. It is also troubling that the procedure did not produce uniform level of safety for all spans. The method should not be used for larger span frames.

In terms the configuration of the frames: (1) it seams that ULS from fundamental loads is the controlling check, with (2) SLS check being significant for hinged frames in very strong earthquake regions. ULS check from the earthquake combination has not been critical for these frames.

The failing configurations have also been recalculated using the global nonlinear analysis method. Case 2.6 and 3.25 formed the first plastic hinge at the load that was (multiplied with reduction factor) smaller than the design load and vertical serviceability limit was slightly exceeded in Case 2.8. Calculation confirmed that the ultimate load-carrying capacity (the highest load) is higher than the design load in all cases.

The detailed analysis of these configurations is presented in the next chapters.

4.2 Details of Case 2.6

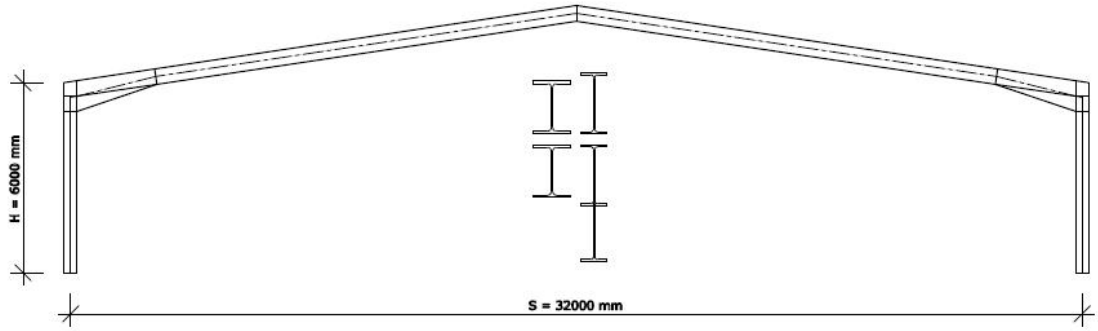

Figure 6. Column HEA450, Rafter IPE500, Fixed base.

In this case the general method ultimate limit state check failed. The frame out-of-plane stability calculation called for low reduction factor (see below).

Out-of-plane critical amplifier: $\alpha_{cr,op} = 1{,}59$

Ultimate plastic amplifier: $\alpha_{ult} = 1{,}51$

Overall reduction factor: $\chi_{op} = 0{,}614$.

Following diagrams show that the first plastic hinge formed already at the lower load level. Method 1 is the global non-linear analysis with all required imperfections and Method 2 is general method, where pushover results were calculated on the wire model without out-of-plane stability effect.

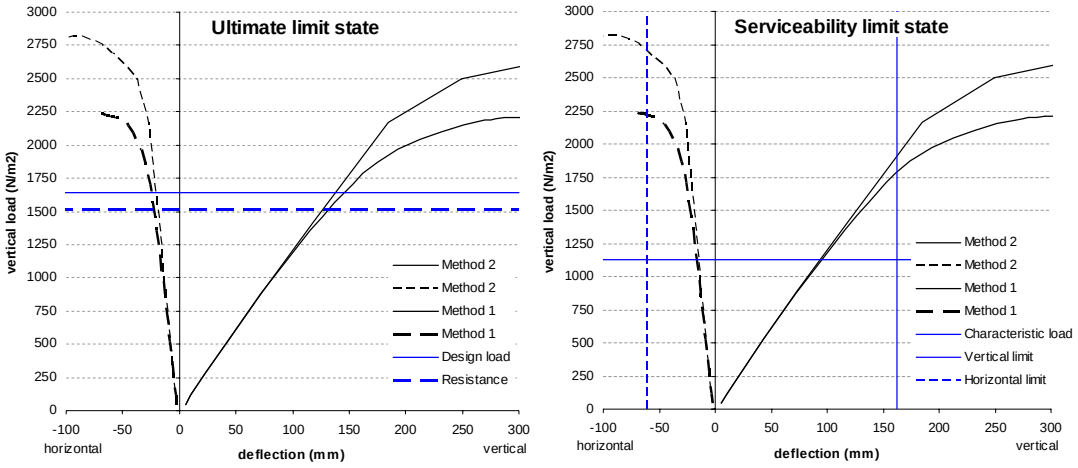

Figure 7. Load-deflection relationship.

4.3 Details of Case 2.8

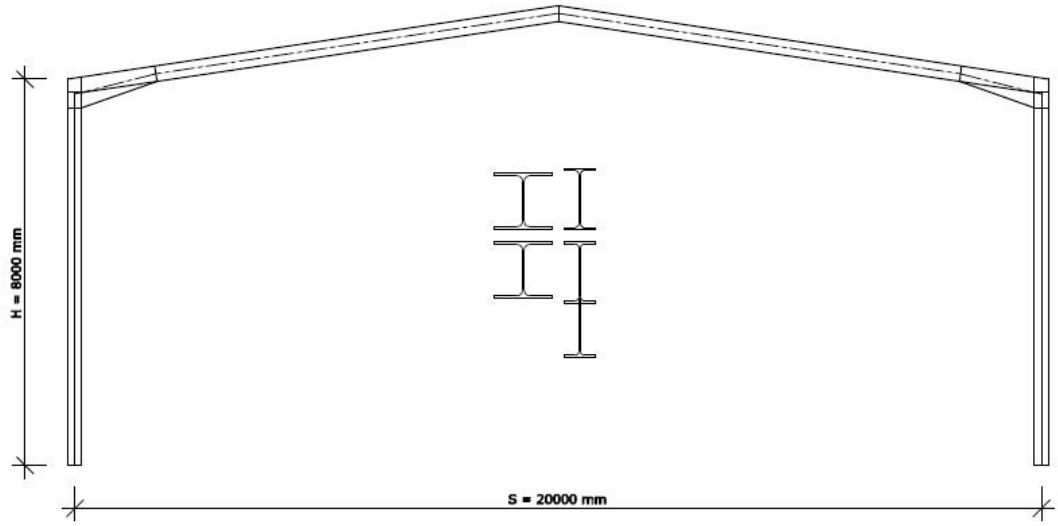

Figure 8. Column HEA320, Rafter IPE330, Fixed base.

Load-deflection diagrams below show that when the characteristic load was reached, the vertical deformation already exceeded the vertical limit (100 mm).

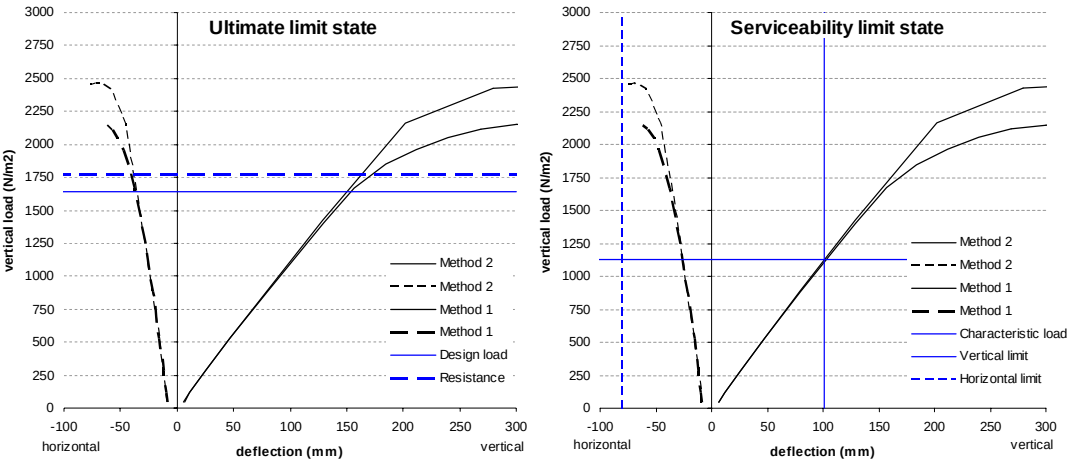

Figure 9. Load-deflection relationship.

4.4 Details of Case 3.25

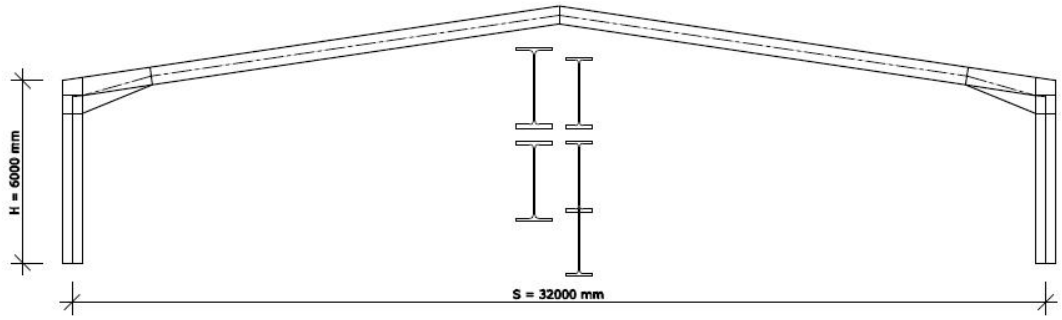

Figure 10. Column HEA700, Rafter IPE600, Pinned base.

In this case the general method ultimate limit state check failed. The frame out-of-plane stability calculation called for low reduction factor (see below).

Out-of-plane critical amplifier:	$\alpha_{cr,op} = 1{,}61$
Ultimate plastic amplifier:	$\alpha_{ult} = 1{,}38$
Overall reduction factor:	$\chi_{op} = 0{,}645$.

Following diagrams show that the first plastic hinge formed already at the lower load level.

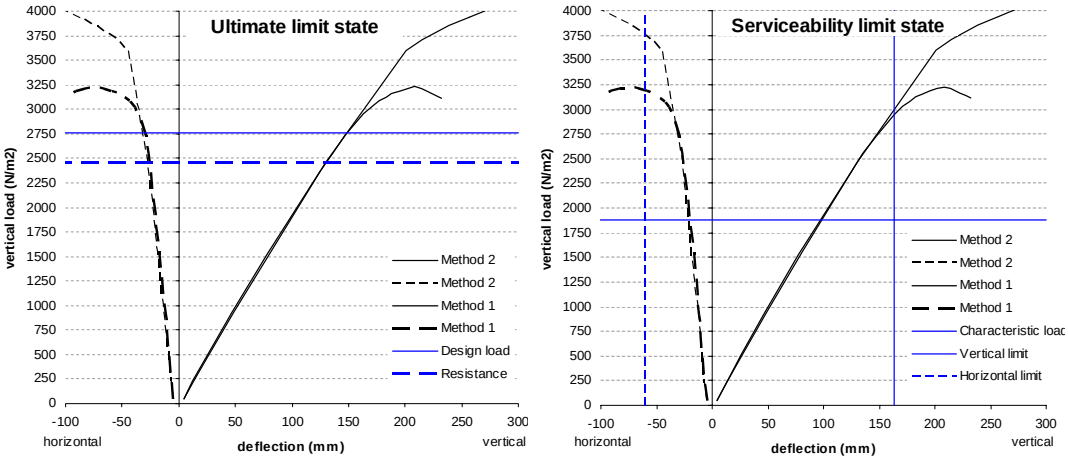

Figure 11. Load-deflection relationship.

5 Optimization results

Several selected cases suggested in the preliminary calculations [11] were optimized for the minimum weight.

Optimized variables:
Column: HE basic beams (HEA, HEB, HEAA)
Rafter: IPE basic beams

As a result we selected the lightest frame from the optimization and another one to make sure that at least one of the suggested frames has HEA profiles as columns.

Table 6. Selected cases.

Case	Span	Snow load	Acceleration (PGA)	Base support
1.2	20 m	750 N/m^2	0,32 g	Fixed
3.20	16 m	1500 N/m^2	0,08 g	Pinned
3.25	32 m	1500 N/m^2	0,08 g	Pinned

Optimization constants:
Height: 6 m
Distance between frames: 6 m
Haunch length: 9.1 % (1/11) of span S, 18.2 % (1/5.5) of half-span L
Roof angle: 15.0 % (8.53°)
Dead load: 380 N/m^2
Wind load: 30 m/s, terrain type 2 (only in fundamental load combinations)
Seismic load: spectrum type 1, ground type B, q = 1.5
Material: S275 with strain hardening

Design situations (EN 1990):
Persistent and transient design situation with dead, snow and reduced wind load
Seismic design situations with seismic, dead and reduced snow load

The weight of the frame optimized for persistent/transient design situation was always higher than the one resulting from seismic optimization. However, it was necessary to check those configurations for all load combinations. E.g. in Case 1.2 the lightest frame resisting both load scenarios had bigger weight than each of the optimized results.

Design method (EN 1993-1-1):
General method: Linear or nonlinear in-plane analysis with global reduction for out-of-plane stability using beam model with stepped cross-sections and shell model

Optimization parameters:
Number of generations: 40
Population size: 40

Optimization methods:
Selection operator: tournament selection
Crossover operator: simulated binary crossover (SBX)

Mutation operator: polynomial mutation

Table 7. Optimization of selected single-span portal frames (40 generations × 40 individuals).

Case	Span	Design situation	The best individual frame				Another suggested frame			
			Column	Rafter	Haunch	Weight	Column	Rafter	Haunch	Weight
1.2	20 m fixed	Seismic	HE450AA	IPE270	L/5.5	2.30 t	HE360A	IPE300	L/5.5	2.57 t
		Persistent/ Transient	HE280A	IPE360	L/5.5	2.44 t	HE340AA	IPE360	L/5.5	2.51 t
		Combination*	**HE300A**	**IPE360**	**L/5.5**	**2.63 t**	(checked also for the seismic situation)			
3.20	16 m pinned	Seismic	HE300AA	IPE330	L/5.5	1.99 t	HE280A	IPE330	L/5.5	2.03 t
		Persistent/ Transient	HE300A	IPE360	L/5.5	2.35 t	HE280A	IPE400	L/5.5	2.37 t
		Combination*	**HE300A**	**IPE360**	**L/5.5**	**2.35 t**				
3.25	32 m pinned	Seismic	HE600AA	IPE550	L/5.5	5.82 t	HE500A	IPE550	L/5.5	6.15 t
		Persistent/ Transient	HE650A	IPE750	L/5.5	7.57 t	HE900AA	IPE750	L/5.5	7.73 t
		Combination*	**HE650A**	**IPE750**	**L/5.5**	**7.57 t**	(IPE750x137 used)			

* Note: The configurations from pre-design [11] were: Case1.2 - HEA300A & IPE360, Case 3.20 - HEA 340 & IPE360, Case 3.25 - HEA 700 & IPE 600.

Table 8. Optimization of selected single-span portal frames (40×40 in the fundamental, and 30×30 in the earthquake load combinations).

Frame weight and feasibility distribution in calculated frames	Fitness development during the run
Case 1.2 Seismic design situation	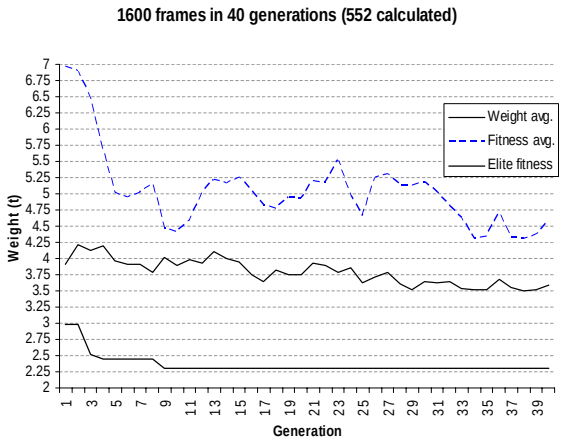
Case 1.2 Persistent/Transient design situation	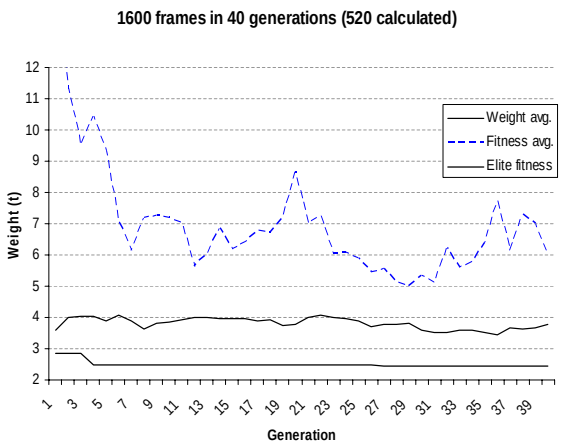

Case 3.20
Seismic design situation

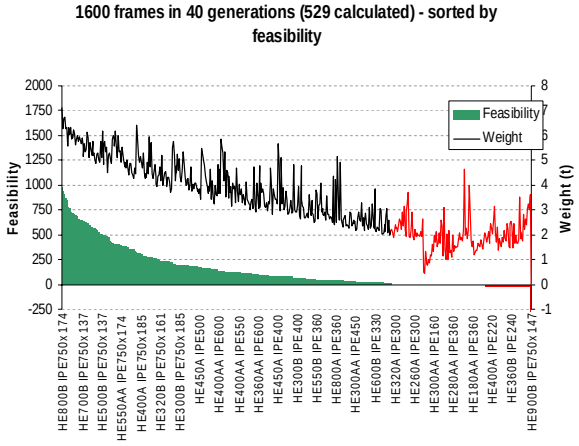

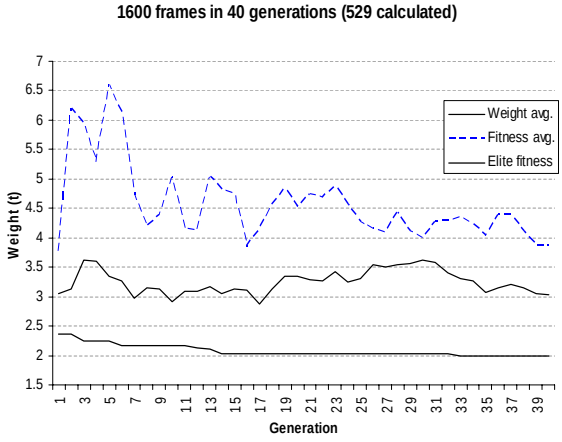

Case 3.20 Persistent/Transient
design situation

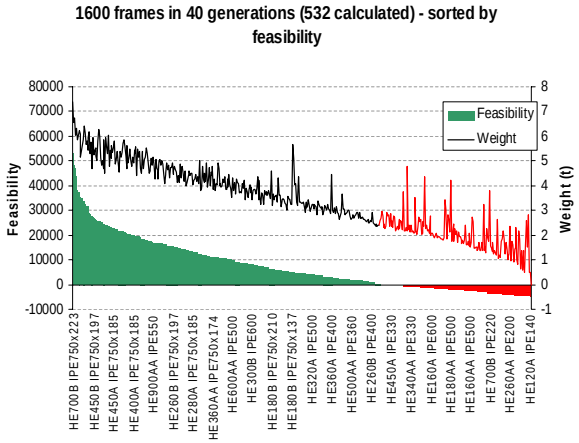

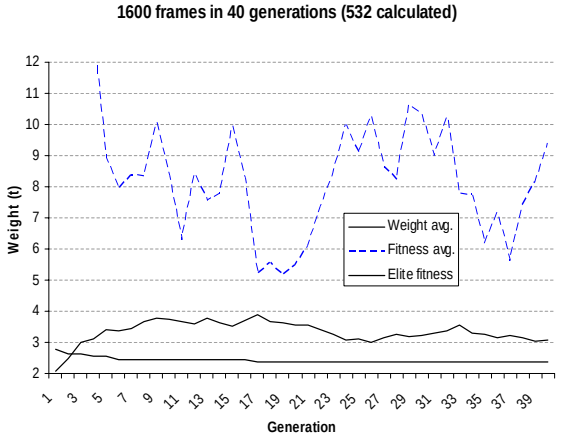

Case 5.3
Seismic design situation

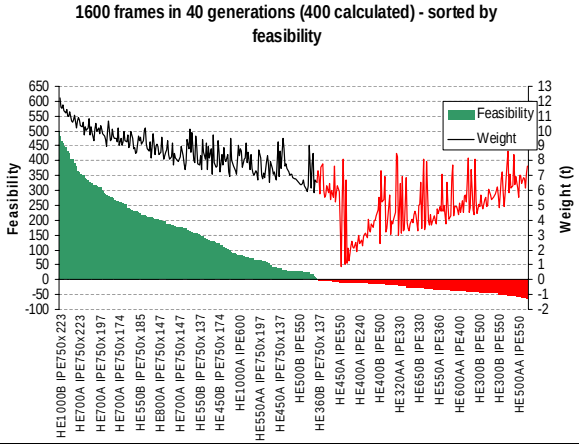

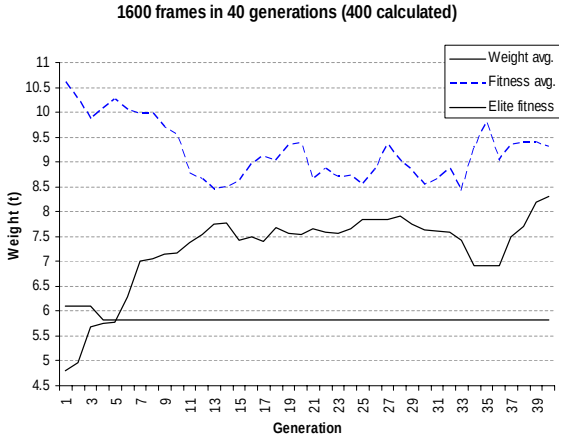

Case 5.3 Persistent/Transient
design situation

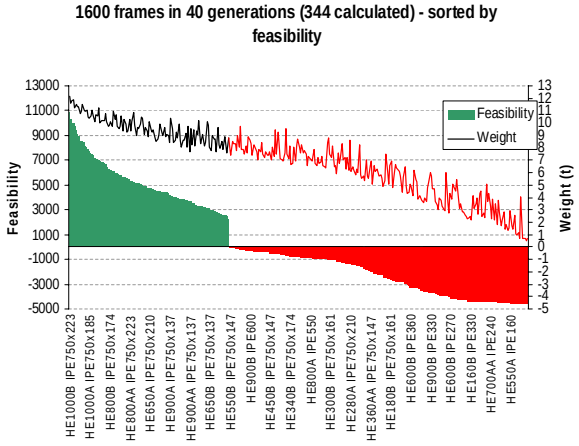

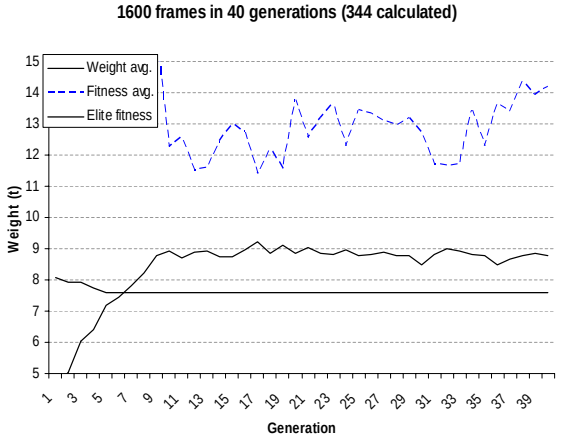

6 Benchmarking selected optimization results

In the following study we used optimization to verify results published in The Structural Engineer [14]. The comparative cost analysis uses Universal Beams as hot-rolled columns and BS standards for load and resistance calculations. In that analysis the most lightweight frame was selected based on the assumption that the moment of inertia of column should be approximately three times the moment of inertia of rafter in case of fixed support. Using our tool we showed that we can decrease the column weight when optimizing in full range of profiles.

Table 9. Basic settings of the comparative study.

	Universal Beams and BS standards [14]	IPE profiles and EC3 General method
Span/Height	14,4/5 m, 18/5,25 m, 21,6/5,5 m, 25,2/5,75 m, 28,8/6 m, 39,6/6,75 m, 43,2/7 m	
Purlin spacing	1,8 m	1,7 to 1,9 m
Roof loading	1,05 kN/m^2	Dead load: 0,30 kN/m^2 Snow load: 0,75 kN/m^2
Wind speed	peak 46 m/s	basic 30 m/s terrain category 1
Steel grade	steel grade 43	S275
Base support	Fixed	
Roof pitch	span/20 (5,7 º)	
Geometric limits and assumptions	min. 50 mm profile legs min. 6 mm steel thickness average column moment of inertia is 3 times rafter moment of inertia	IPE, IPE A, IPE O, IPE R, IPE V from 100 to 750 mm height, section class max. 3
Knee haunches	span/8	
Loading standards	BS 6399 *"Design loading for buildings"*	Eurocode 1
Design standards	BS 449 *"The use of structural steel in buildings"*	Eurocode 3: General method

For the optimization we used 40 generation with population of 40 frames in each generation (40×40). Considering the number of possible combinations of profiles this setting cannot guarantee the absolute optimum in all cases (e.g. the 18 m span calculation shows that the rafter can be further optimized), but still produce results that confirmed the proper steel consumption in rafters and a constantly growing difference in column weight.

Table 10. Optimized steel consumption.

Geometry		Universal Beams and BS standards [14]				IPE profiles and EC3 General method			
Span (m)	Height (m)	Rafter		Column		Rafter		Column	
		Profile	kg/m	Profile	kg/m	Profile	kg/m	Profile	kg/m
14.4	5.00	UB254x146x31	31.1	UB356x171x45	45	IPE200R	26.6	IPE330A	42.9
18.0	5.25	UB305x127x37	37	UB406x178x60	60	IPE360	57.1	IPE330A	42.9
21.6	5.50	UB356x171x45	45	UB457x191x74	74	IPE330	49.1	IPE400A	57.4
25.2	5.75	UB406x178x54	54	UB533x210x92	92	IPE400A	57.4	IPE400O	75.7
28.8	6.00	UB457x191x67	67.1	UB610x229x101	101.2	IPE450A	67.1	IPE500A	79.2
32.4	6.25	UB457x191x74	74	UB686x254x125	125	IPE450A	67.1	IPE600A	107.5
36.0	6.50	UB533x210x82	82	UB762x267x147	147	IPE500A	79.3	IPE600A	107.5
39.6	6.75	UB533x210x92	92	UB762x267x173	173	IPE500A	79.3	IPE750x137	137.4
43.2	7.00	UB610x229x101	101	UB838x292x176	176	IPE550A	91.8	IPE750x137	137.4

Unfortunately, we could not compare the weight of the structure directly because the methodology of evaluating the weight of the frames was not published in the comparative cost calculation paper [14], and it probably includes other parts of the structure (e.g. purlins, stiffeners, columns base plate, wind bracing, etc.). Therefore, a comparison of the cross-sectional mass level has been performed, and is presented in Figure 12.

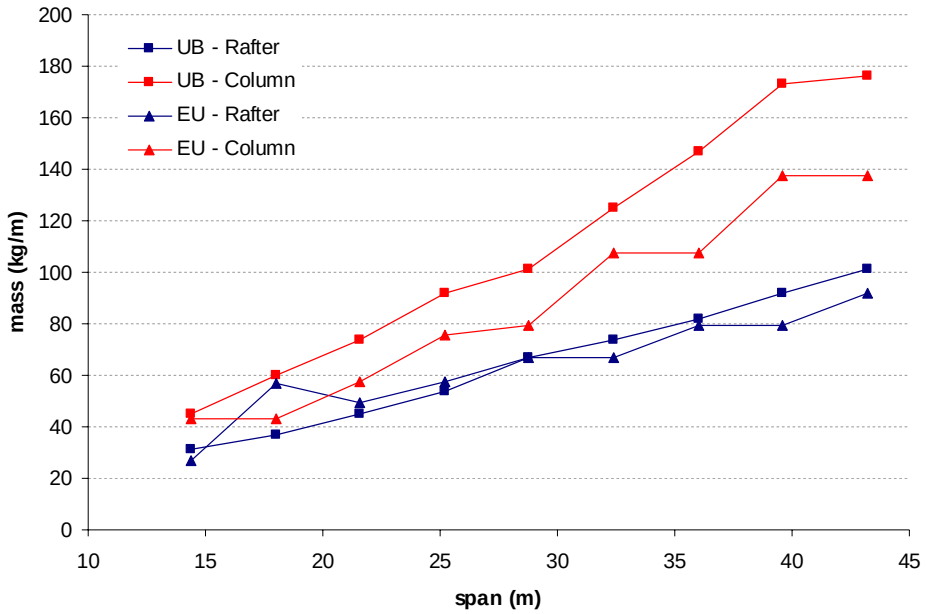

Figure 12. Optimized steel consumption on columns and rafters using universal beams (UB) and IPE (EU) hot-rolled profiles.

7 Conclusions

The results of portal frame design and optimization are presented in this report. We investigated HR and TW frames and we used three alternative design methods (GNLA, GMA and IFM), varying in sophistication and required analysis time. All three design methods conform to design codes used in Europe, i.e. [6], [7], [8], [9], [10].

One of the conclusions in the design phase of the frames was that the pre-design of the frames, carried out the University of Thessaly [11], produced generally conservative frame configurations. The degree of conservatism was decreasing with the span of the frames from 40 - 50% at 16m span to 0 - 5% for 32m spans. This variation of the degree of conservativeness shows that the pre-design procedure was not working well for slender frames.

We also observed the difficulty of applying the IFM when it came to evaluating the slenderness of members and the corresponding buckling reduction factor. The effect of slenderness was less important for short spans, reducing the possibility to misevaluate the load capacity. However, as slenderness increases with larger spans, the proper evaluation of the member slenderness becomes the key question of the design. In these cases the IFM methods leaves many occasions for design error.

GMA presents good balance between required design effort and accuracy of the results. We benchmarked GMA based results with earlier reports [14] , finding good correlation. GMA has good sensitivity to slenderness due to the incorporated buckling analysis, and the support conditions frames can be represented accurately (e.g. eccentric translational supports). Hence, the many controversial “support assumptions” used in the IFM are eliminated. The disadvantage of the GMA method is, that it tries to “lump” the slenderness properties of the frame into one number (i.e. a global reduction factor). This can be less accurate then having separate reduction factors for each member (IFM). In our experience, this disadvantage causes much less problems to the designer, then coming up with procedures to predict the slenderness of members in the IFM. Also, the GMA method is always conservative if the supports are properly represented, unlike the IFM where a few “engineering assumptions” can easily lead to unconservative design.

The GNLA method is very costly in terms of computing time. Therefore, in our studies it has been used only as comparison basis for the GMA and IFM designs. We assumed that the GNLA is the method which can predict most accurately the capacity of the frames, even if use of the large imperfections suggested by EN 1993 [9] can seem controversial. As a note, one should remember that these imperfections are “equivalent geometric imperfections”, meant to account for the imperfections of the real structure, geometric but also residual stresses. One major disadvantage of the GNLA, in our implementation, is that we can not perform plastic design, as the concept of “plastic hinge” is not interpretable on the shell models used for GNLA. This leaves the GNLA with some conservativeness too especially in HR frames.

All three methods seem to perform well in the genetic algorithm (GA) optimization context of large number of repeated runs. During the GA runs many disproportionate frames are created and analysed. These frames are later eliminated during the selection process, but it is the nature of the GA algorithm to produce these frames, as it is trying to screen the design space for the optimal configuration.

One problem for such disproportionate configurations in GMA and GMLA, is that they tend to require very finer meshing in FEM, therefore resulting in large models slowing down the analysis. It is possible, for speeding up analysis, to set geometrical limits for frames. The disadvantage of using such limits is that the search space becomes narrower, some configurations being a priory excluded.

In terms the optimal frame configurations, especially focusing on the HR configurations calculated in this study:

- It seems that ULS from fundamental loads is the controlling check for almost all our frame configurations (Table 5).

- The horizontal SLS check is significant for hinged frames, in very strong earthquake regions with PGA = 0.32g. ULS check from the earthquake combination has not been critical for these frames.

References

[1] TIMOSHENKO S.P., GERE J.M. *Theory of elastic stability*, 2nd edition, London, 1961.

[2] ŠAPALAS, V., SAMOFALOV, M., VIAČESLAVAS, Š FEM stability analysis of tapered beam-columns, *Journal of Civil Engineering and Management*, 2005, Volume XI., No. 3, 211-216.

[3] LÓPEZ A., YONG D.J., SERNA M.A., Lateral-torsional buckling of steel beams: a general expression for the moment gradient factor, *Stability and ductility of steel structures*, Lisbon, Portugal, 2006.

[4] DAVIES J. M., Inplane stability in portal frames, *The Structural Engineer*, Volume 68, No. 8, April 1990.

[5] FÜLÖP L., BEAUCAIRE P, Advanced analysis of the performance of steel frames, *VTT Research report*, Espoo, Finland, 2009.

[6] EN 1990:2002, Eurocode: Basis of structural design.

[7] EN 1991-1-4:2005, Eurocode 1: Actions on structures - Part 1-4: General actions - Wind actions.

[8] EN 1991-3:2006, Eurocode 1: Actions on structures - Part 3: Actions induced by cranes and machinery.

[9] EN 1993-1-1:2005, Eurocode 3: Design of steel structures - Part 1-1: General rules and rules for buildings.

[10] EN 1998-1:2004, Eurocode 8: Design of structures for earthquake resistance - Part 1: General rules, seismic actions and rules for buildings.

[11] VARELIS, D. VASILIKIS, S. KARAMANOS, P. TSINTZOS: WP2: Performance analysis of selected steel types for one-storey industrial buildings, Research report.

[12] JENKINS, D., *Frame analysis with Excel*, http://newtonexcelbach.wordpress.com/, Interactive Design Services Pty Ltd., Sydney, Australia, 2009.

[13] ASWANDY, R. GREINER, “Design of Members under Bending and Axial Compression with Intermediate Lateral Restraints,” Maastricht: 2005.

[14] J. HORRIDGE and L. MORRIS, “Comparative costs of single-*storey steel framed stru*ctures,” *The Structural Engineer*, vol. 64A, Jul. 1986, pp. 177 - 181.

[15] KING, C. M., SCI P164 Technical Report: *Design of steel portal frames for Europe*, The Steel Construction Institute, 2001, ISBN 1 85942 054 0

Annex A: Benchmark calculation

Frame configuration

Geometry

$S = 20\ m + h_{column} = 20{,}2\ m$ (span of the frame)

$H = 6\ m$ (eaves height)

$T = 6\ m$ (distance between frame centres)

$\alpha = 15\%$ (roof pitch)

$L_h = S / 5.5$ (length of the haunch)

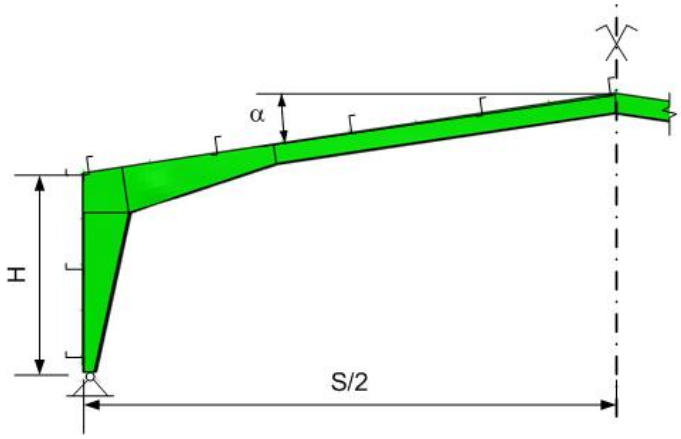

Cross-sections

$h_{beam} = 400\ mm$

$h_{haunch} = 800\ mm$

$h_{column} = 200\ mm$

$b = 260\ mm$

$t_f = 10\ mm$

$t_w = 8\ mm$

Characteristic vertical loads

$P_{dead} = 0.38\ kN/m^2$ (including purlins and self-weight estimation)

$P_{snow} = 0.75\ kN/m^2$

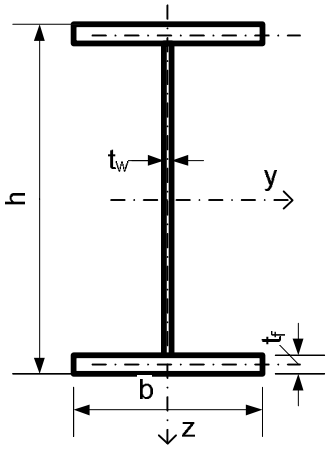

Material properties

$f_y = 275\ MPa$

$E = 210000\ MPa$

$G = 81000\ MPa$

Purlins

$h_{purlin} = 240\ mm$ (purlin height)

$a_{beam} = 1.23\ m$ (distances between purlins)

$a_{column} = 1.29\ m$ (distances between side rails)

Points of calculation

A	apex cross-section
B	beam - end of the haunch
C_1	corner section of the beam
C_2	corner section of the column
D	column - base support section

Ultimate limit states calculated at the design load level 1640 N/m^2				
		Method 1 Global analysis	**Method 2 General method**	**Method 3 Member checks**
Structural limits		Internal stress exceeds yield strength		ULS interaction formulae and shear check
		vertical deflection $u_{\lim} = 100\ mm$ horizontal deflection $v_{\lim} = 60\ mm$		
Global stability		Sway imperfections 21.2 mm		
In-plane member stability		Bow imperfections 25.5 mm	In-plane bow imperfections 40.4 mm	Reduction factors 0.892 (beam) 0.960 (column)
Out-of-plane member stability			Overall reduction factor 0.549	in compression 0.293 (beam) 0.653 (column) in bending 0.497 (beam) 0.389 (column)
In-plane critical amplifier		3.49	27.0	19.1
Out-of-plane critical amplifier			3.49	n/a
Order of calculation		2nd order	2nd order	1st order
Axial forces	A	n/a	55.4 kN	54.8 kN
	B		68.2 kN	67.9 kN
	C_1		68.5 kN	74.2 kN
	C_2		99.4 kN	99.8 kN
	D		102 kN	99.8 kN
Bending moments	A	n/a	-97.0 kNm	-92.2 kNm
	B		68.1 kNm	62.5 kNm
	C_1		271 kNm	256 kNm
	C_2		272 kNm	267 kNm
	D		0.00 kNm	0.00 kNm
Shear forces	A	n/a	2.68 kN	8.49 kN
	B		55.0 kN	55.4 kN
	C_1		84.1 kN	84.3 kN
	C_2		55.3 kN	55.7 kN
	D		50.8 kN	50.2 kN
Extreme fibre normal stresses	A	n/a	89.5 MPa	n/a
	B		66.4 MPa	
	C_1		102.1 MPa	
	C_2		105.2 MPa	
	D		15.4 MPa	
ULS Capacity		**2800 N/m^2**	**2272 N/m^2**	**1761 N/m^2**

Serviceability limit states calculated at the characteristic load level 1130 N/m^2				
		Method 1 Global analysis	**Method 2 General method**	**Method 3 Member checks**
Initial deformation		Sway and bow imperfections	Sway and in-plane bow imperfections	Only sway imperfections
Vertical deflections	A	39.3	33.1 mm	33.5 mm
	B		10.9 mm	10.5 mm
	C_1		0.4 mm	0.6 mm
	C_2		0.1 mm	0.3 mm
	D		0.0 mm	0.0 mm
Horizontal deflections	A	5.50	1.0 mm	0.4 mm
	B		4.2 mm	3.7 mm
	C_1		6.3 mm	6.5 mm
	C_2		6.7 mm	7.7 mm
	D		0.0 mm	0.0 m
SLS Capacity		**3088 N/m^2**	**3359 N/m^2**	**3410 N/m^2**

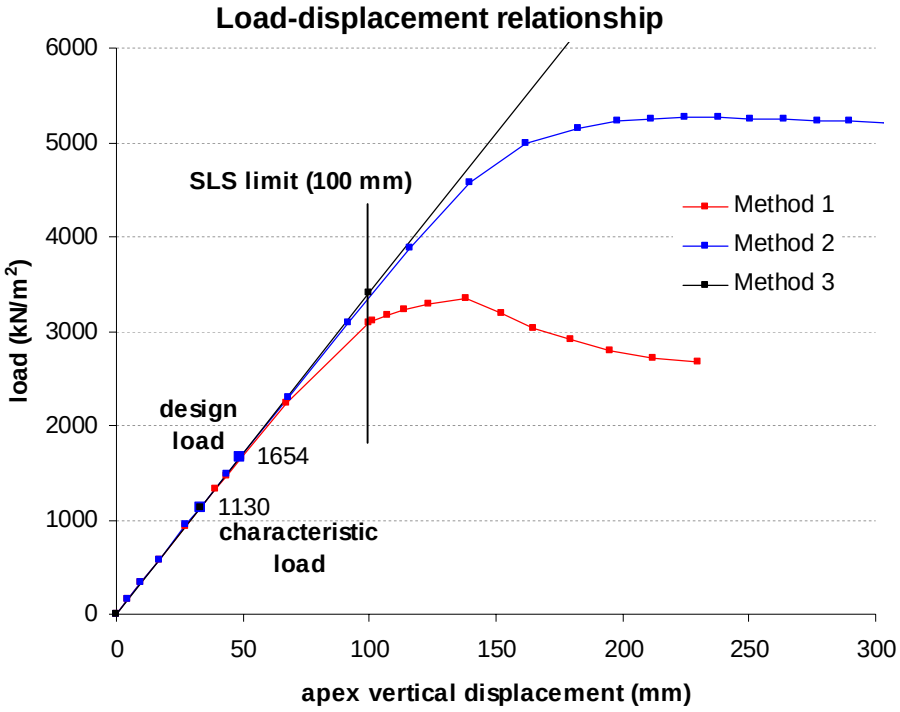

Figure 13. Load-displacement comparison of used methods.

Method 1: Global analysis - detailed calculation

Loading (EN 1991)

The rafter is loaded with vertical point loads at each purlin

$F_{des} = P_{des} a_{beam} T$ and $0.5 F_{des}$ at the eaves.

The load level P gradually increases until the frame collapse P_{max} while internal stresses are measured at the design load level. In the **vertical pushover analysis**

snow load is considered to be the leading variable action and a combination of actions for **persistent or transient design situation** (fundamental combination) is calculated as follows:

$$P_{des} = \gamma_{G,\sup} P_{dead} + \gamma_S P_{snow} = 1.64\ kN/m^2 \quad \text{(EN 1990 6.10)},$$

and deflections are measured at the characteristic load level

$$P_{char} = P_{dead} + P_{snow} = 1.13\ kN/m^2 .$$

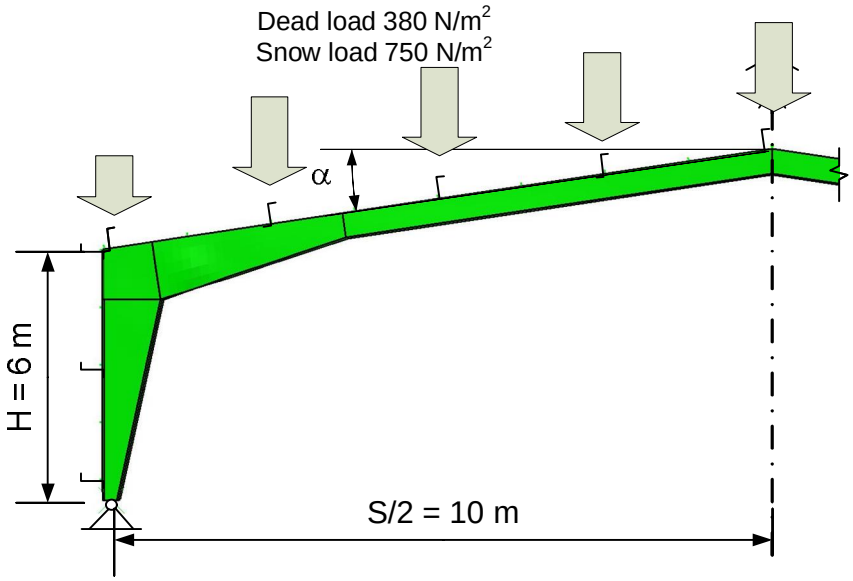

Figure 14. Loading of the frame.

Imperfections for global analysis of frames (EN 1993-1-1, 5.3.2)

The appropriate sway imperfection is applied as increment to each node x-coordinate:

$$x_{imp} = x + y \cdot \tan\phi ,$$
$$x_{imp} = 21.2\ mm \quad \text{at frame corner, where} \quad y = 6000\ mm$$

where $\phi = \dfrac{\alpha_h \alpha_m}{200} = 0.00356$ (EN 1993-1-1, 5.3.2)

$$\alpha_h = \max\left(\frac{2}{3}; \min\left(1; \frac{2}{\sqrt{H}}\right)\right) = 0.816 \quad \text{(EN 1993-1-1, 5.5)}$$

$$\alpha_m = \sqrt{0{,}5\left(1 + \frac{1}{m}\right)} = \sqrt{0.75} = 0.866 \quad \text{for } m = 2 \text{ columns.}$$

Initial bow imperfections for buckling curve c (out-of-plane buckling)

$$e_0 = 0.5\frac{L}{200} = 0.5\frac{(0.5S)/\cos\alpha}{200} = 25.5\ mm$$

Critical load

We received the first buckling mode with positive load amplifier from the linear eigenvalue analysis (LEA) on 3D shell model. The critical load amplifier is:

$$\alpha_{cr} = 3.4889$$

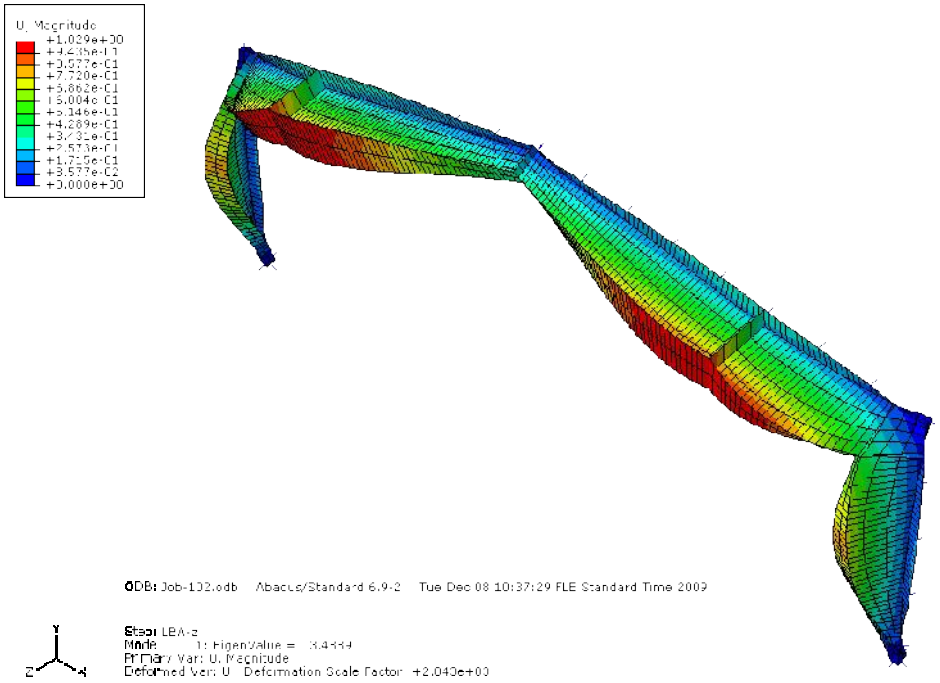

Figure 15. The first buckling shape.

Imperfections were scaled to 25.5 mm and used in the pushover calculation together with sway imperfections 21.2 mm.

Pushover analysis

The perturbed 3D shell model was loaded with increasing load (Riks step in Abaqus) as so called Geometrically and Materially Non-linear Analysis on Imperfect Structure (GMNIA).

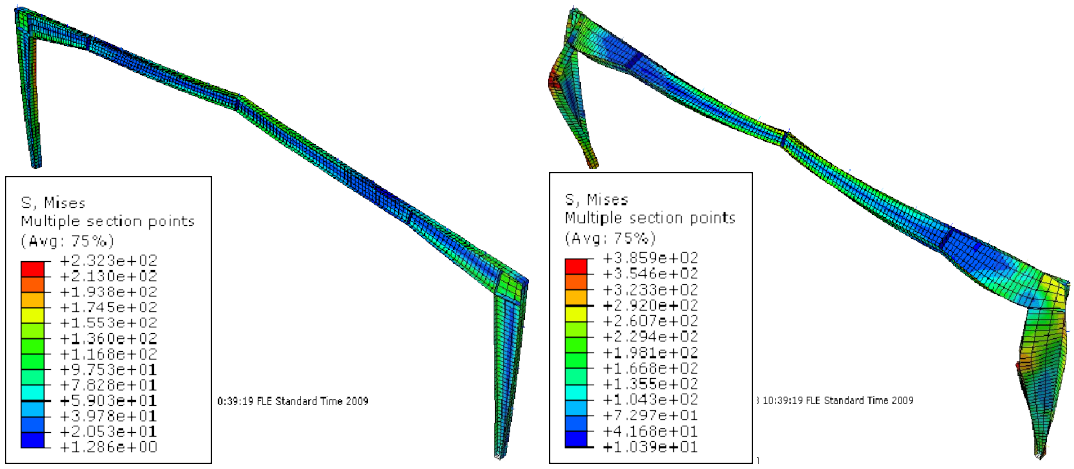

Figure 16. Stress and deformation at the design load level (left) and at the ultimate load (right).

Method 2: General method (EN 1993-1-1, 6.3.4) - detailed calculation

Loading and imperfections (EN 1991 and EN 1993-1-1, 5.3)

We used the same loading and sway imperfections as in the previous analysis. This time it was applied to beam model (wire elements).

Initial bow imperfections for buckling curve b (in-plane buckling)

$$e_0 = \frac{L}{250} = \frac{(0.5S)/\cos\alpha}{250} = 40.4\ mm\,.$$

In-plane critical load

We received the first buckling mode with positive load amplifier from the linear eigenvalue analysis (LEA) on 2D beam model. The critical load amplifier is:

$$\alpha_{cr} = 27.005$$

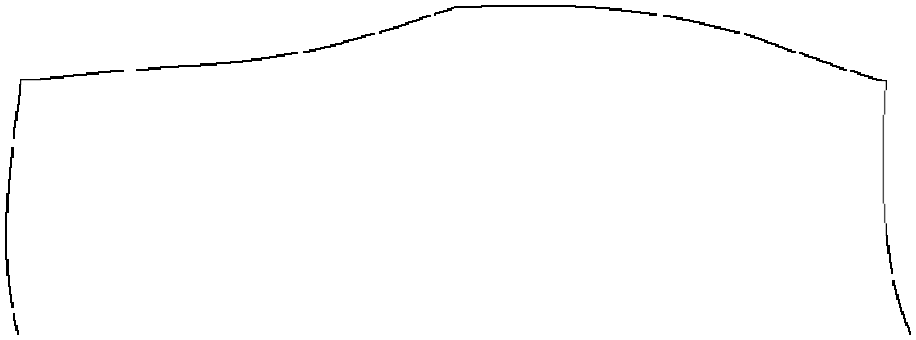

Figure 17. The first in-plane buckling mode.

In-plane imperfections were scaled to 40.4 mm and used in the pushover calculation together with sway imperfections 21.2 mm.

Pushover analysis

The perturbed 2D beam model was loaded with increasing load (Riks step in Abaqus) as so called Geometrically and Materially Non-linear Analysis on Imperfect Structure (GMNIA).

The minimum load amplifier of the design loads to reach the characteristic resistance of the most critical cross-section without taking out-of-plane buckling into account is:

$$\alpha_{ult,k} = 2.5275$$

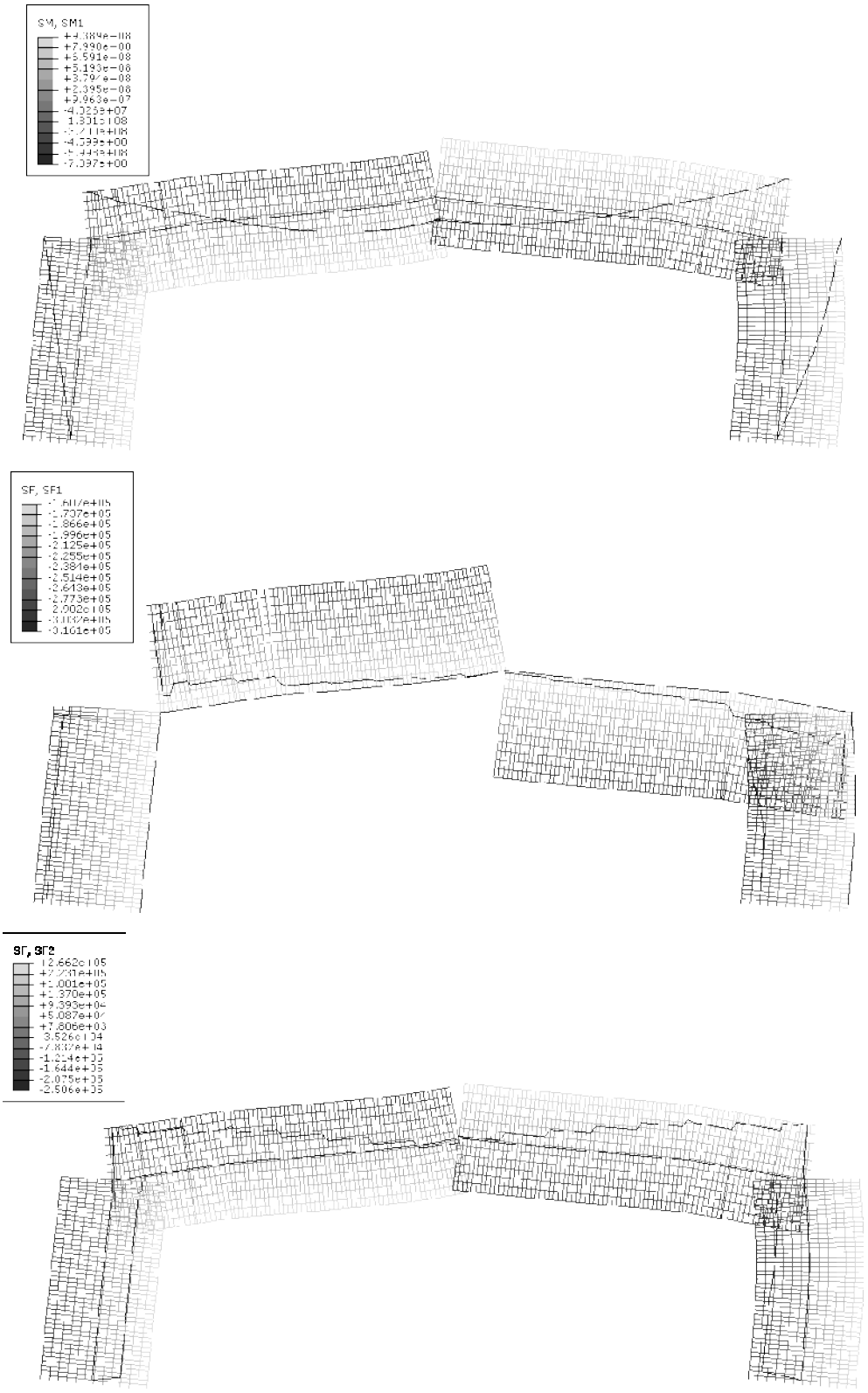

Figure 18. Internal forces at the ultimate load level: Bending moments (top), Axial froces (middle), Shear forces (bottom).

Out-of-plane critical load

The first positive out-of-plane buckling mode was calculated on the 3D shell model. Its eigenvalue is the same as in the previous calculation (Method 1). The

minimum load amplifier of the design loads to reach the elastic critical resistance with regards to lateral or lateral torsional buckling is

$$\alpha_{cr,op} = 3.4889$$

General method calculation

The reduction factor was calculated using EC3 buckling curve “d” and the global non-dimensional slenderness for out-of-plane buckling:

$$\bar{\lambda}_{op} = \sqrt{\frac{\alpha_{ult,k}}{\alpha_{cr,op}}} = 0.851$$

$$\phi_{op} = 0{,}5\left[1 + \alpha\left(\bar{\lambda}_{op} - 0{,}2\right) + \bar{\lambda}_{op}^2\right] = 1.110\,,$$

where $\alpha = 0.76$

$$\chi_{op} = \frac{1}{\phi_{op} + \sqrt{\phi_{op}^2 - \bar{\lambda}_{op}^2}} = 0.549\,.$$

Overall resistance of the structural component can be verified using following condition:

$$\chi_{op}\alpha_{ult,k} / \gamma_{M1} = 1.388 \geq 1{,}0$$

Method 3: Member checks (EN 1993-1-1) - detailed calculation

Loading and imperfections (EN 1991 and EN 1993-1-1, 5.3)

The rafter is loaded with equally distributed vertical load (dead load, snow):

$$P_{des} = \gamma_{G,\sup} P_{dead} + \gamma_S P_{snow} = 1.64\ kN/m^2 \approx 9.83\ kN/m \quad \text{(EN 1990 6.10)},$$

where $\gamma_{G,\sup} = 1.35$, $\gamma_S = 1.5$

and $P_{char} = P_{dead} + P_{snow} = 1.13\ kN/m^2 \approx 6.78\ kN/m$ for serviceability limit state.

The appropriate sway imperfection is applied as increment to each node x-coordinate:

$$x_{imp} = x + y \cdot \tan\phi\,,$$

where $\phi = \frac{\alpha_h \alpha_m}{200} = 0.00356$ (EN 1993-1-1, 5.3.2)

$$\alpha_h = \max\left(\frac{2}{3}; \min\left(1; \frac{2}{\sqrt{H}}\right)\right) = 0.816 \text{ (EN 1993-1-1, 5.5)}$$

$$\alpha_m = \sqrt{0.75} = 0.866.$$

Internal forces and cross-sectional resistances (EN 1993-1-1)

	Internal forces		
	axial forces N_{Ed}	bending moments $M_{y,Ed}$	shear forces $V_{z,Ed}$
A: beam apex	54.8 kN	-92.2 kNm	8.49 kN
B: beam constant part	67.9 kN	62.5 kNm	55.4 kN
C_1: beam corner	74.2 kN	256 kNm	84.3 kN
C_2: column corner	99.8 kN	265 kNm	55.7 kN
D: column support	99.8 kN	0.00 kNm	50.2 kN
	Cross-sectional resistances		
	$N_{Rk} = A \cdot f_y$	$M_{y,Rk} = W_{el,y} \cdot f_y$	$V_{z,Rk} = A_V \cdot f_y / \sqrt{3}$
A, B: beam	227 kN	322 kNm	483 kN
C: corner	315 kN	775 kNm	991 kN
D: column support	183 kN	140 kNm	229 kN

In plane critical multiplier (Davies [4])

$$\alpha_{cr} = \frac{3E\, I_{y,B}}{s\left(N_{Ed,D} h + 0{,}3 N_{Ed,B} s\right)} = 19.1$$

where s, h are lengths of rafter and column

$$R = \frac{I_{y,D} s}{I_{y,B} h} = 0.377$$

The first order elastic analysis is carried out because $\alpha_{cr} > 10$.

Critical loads

a) In-plane flexural buckling

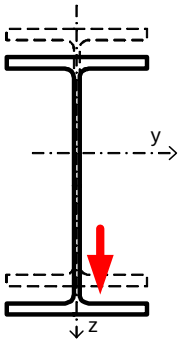

Equivalent moments of inertia are (CTICM):

For beam: $I_{y,eq,beam} = \dfrac{1}{3\left(\dfrac{\lambda_1^3}{I_{y,C} X_1} + \dfrac{\lambda_2^3}{I_{y,B} X_2}\right)} = 490 \cdot 10^6 mm^4$

where $\lambda_1 = \dfrac{L_h}{L_{beam}} = 0.337$, $\lambda_2 = \dfrac{L_{beam} - L_h}{L_{beam}} = 0.663$

$$X_1 = \frac{1}{\frac{(1+\delta_1)^2}{\xi_1 - 1} - \frac{\delta_1^2}{\xi_1(\xi_1 - 1)} + \frac{2}{(\xi_1 - 1)^3}(\xi_1 - 1 - [1 + (\xi_1 - 1)(1+\delta_1)]\ln \xi_1)} = 0.082$$

$$\delta_1 = \frac{L_{beam} - L_h}{L_h} = 1.97\,,\ \xi_1 = \sqrt{\frac{I_{y,B}}{I_{y,C}}} = 0.456$$

$$X_2 = \frac{1}{\frac{(1+\delta_2)^2}{\xi_2 - 1} - \frac{\delta_2^2}{\xi_2(\xi_2 - 1)} + \frac{2}{(\xi_2 - 1)^3}(\xi_2 - 1 - [1 + (\xi_2 - 1)(1+\delta_2)]\ln \xi_2)} = 4.65$$

$$\delta_2 = 0.00\,,\ \xi_1 = \sqrt{\frac{I_{y,C}}{I_{y,A}}} = 2.19$$

For column: $I_{y,eq,column} = I_{y,C}\frac{X_1}{3} = 619 \cdot 10^6\, mm^4$

$$X_1 = \frac{1}{\frac{(1+\delta_1)^2}{\xi_1 - 1} - \frac{\delta_1^2}{\xi_1(\xi_1 - 1)} + \frac{2}{(\xi_1 - 1)^3}(\xi_1 - 1 - [1 + (\xi_1 - 1)(1+\delta_1)]\ln \xi_1)} = 1.65$$

$$\delta_1 = 0.00\,,\ \xi_1 = \sqrt{\frac{I_{y,D}}{I_{y,C}}} = 0.456$$

Critical lengths are:

For beam: $L_{cr,y,beam} = L_{beam} = 9.84\ m$

For column: $L_{cr,y,column} = L_{column}\sqrt{\frac{1 - 0.2(\eta_1 + \eta_2) - 0.12\eta_1\eta_2}{1 - 0.8(\eta_1 + \eta_2) + 0.6\eta_1\eta_2}} = 8.78\ m$

where $\eta_1 = \frac{K_c}{K_c + K_{12}} = 0.814$ $\eta_2 = 0.00$

$K_c = \frac{I_{y,eq,column}}{L_{column}} = 109273\ mm^3$ $K_{12} = \frac{I_{y,eq,beam}}{2L_{beam}} = 24890\ mm^3$

Coefficients of variable cross-sections (Šapalas et al. [2]) are

For beam: $\frac{I_{y,\min}}{I_{y,\max}} = \frac{I_{y,B}}{I_{y,C}} = 0.208 \Rightarrow \alpha_n = 0.746$

For column: $\frac{I_{y,\min}}{I_{y,\max}} = \frac{I_{y,D}}{I_{y,C}} = 0.045 \Rightarrow \alpha_n = 0.619$

$\frac{I_{y,\min}}{I_{y,\max}}$	0,01	0,05	0,1	0,2	0,3	0,4	0,5	0,6	0,7	0,8	0,9	1
α_n	0,563	0,629	0,676	0,740	0,788	0,829	0,864	0,895	0,924	0,951	0,976	1

Critical forces are:

For beam: $N_{cr,FBy} = \left(I_{y,C} \frac{L_h}{0{,}5S} \alpha_n + I_{y,B} \frac{0{,}5S - L_h}{0{,}5S} \right) \frac{\pi^2 E}{L^2_{cr,y,beam}} = 9740\ kN$

For column: $N_{cr,FBy} = \alpha_n \frac{\pi^2 E I_{y,C}}{L^2_{cr,y,column}} = 18760\ kN$

b) Out-of-plane flexural buckling (between supports)

Critical lengths are equal to the distance between lateral restraints. Critical forces are:

For beam: $N_{cr,FBz} = \frac{\pi^2 E I_{z,B}}{a^2_{beam}} = 40142\ kN$

For column: $N_{cr,FBz} = \frac{\pi^2 E I_{z,D}}{a^2_{column}} = 36445\ kN$

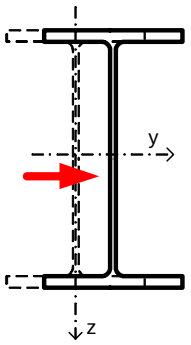

c) Torsional buckling (between supports)

Critical lengths are equal to the distance between lateral restraints. Critical forces are:

Beam: $N_{cr,TB} = \frac{\left(I_{w,B} E\pi^2 / L^2_{cr,z,beam} \right) + GI_{t,B}}{i^2_{0,B}} = 48278\ kN$

Column: $N_{cr,TB} = \frac{\left(I_{w,D} E\pi^2 / L^2_{cr,z,column} \right) + GI_{t,D}}{i^2_{0,D}} = 28603\ kN$

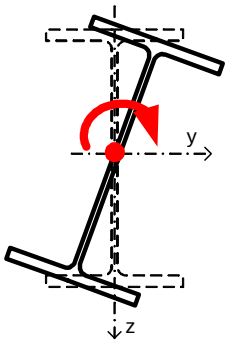

d) Torsional-flexural buckling (eccentrically restrained)

Critical forces calculated from the shallow end are:

For beam: $N_{cr,TFB} = \frac{\left(I_{w,B} + I_{z,B} e^2_{z,B} \right) \left(E\pi^2 / L^2_{beam} \right) + GI_{t,B}}{e^2_{z,B} + i^2_{0,B}} = 947\ kN$

For column: $N_{cr,TFB} = \frac{\left(I_{w,D} + I_{z,D} e^2_{z,D} \right) \left(E\pi^2 / L^2_{column} \right) + GI_{t,D}}{e^2_{z,D} + i^2_{0,D}} = 2378\ kN$

e) Lateral torsional buckling (between supports)

The moment gradient factor estimation is $C_1 = 1.14$.

Critical moments are:

For beam: $$M_{cr} = C_1 \frac{\pi^2 E}{a_{beam}^2} \sqrt{\frac{I_{w,B}}{I_{z,B}} + \frac{a_{beam}^2 GI_{t,B}}{\pi^2 EI_{z,B}}} = 8977 kNm$$

For column: $$M_{cr} = C_1 \frac{\pi^2 E}{a_{column}^2} \sqrt{\frac{I_{w,D}}{I_{z,D}} + \frac{a_{column}^2 GI_{t,D}}{\pi^2 EI_{z,D}}} = 5532 kNm$$

f) Lateral torsional buckling (eccentrically restrained)

Critical forces calculated at the deep end are:

For beam: $$N_{cr,TFB} = \frac{\left(I_{w,C1} + I_{z,C1} e_{z,C1}^2\right)\left(E\pi^2 / L_{beam}^2\right) + GI_{t,C1}}{e_{z,C1}^2 + i_{0,C1}^2} = 787\ kN$$

For column: $$N_{cr,TFB} = \frac{\left(I_{w,C2} + I_{z,C2} e_{z,C2}^2\right)\left(E\pi^2 / L_{column}^2\right) + GI_{t,C2}}{e_{z,C2}^2 + i_{0,C2}^2} = 2241\ kN$$

Equivalent section factors are

For beam: $c = 1 + (c_0 - 1)\sqrt{\frac{L_h}{L_{beam}}} = 1{,}06$ (from table F.2 [15] $c_0 = 1{,}108$)

For column: $c = c_0 = 1{,}43$

Equivalent moment factors are

$$m_t = \frac{1}{12}\left(\frac{M_{c,Rd}}{M_{Sd}}\right)_{\min}\left(\frac{M_{Sd1}}{M_{c,Rd1}} + \frac{3M_{Sd2}}{M_{c,Rd2}} + \frac{4M_{Sd3}}{M_{c,Rd3}} + \frac{3M_{Sd4}}{M_{c,Rd4}} + \frac{M_{Sd5}}{M_{c,Rd5}} + 2\mu_{SE}\right)$$

	For beam		For column	
	M_{Sd}	$M_{c,Rd}$	M_{Sd}	$M_{c,Rd}$
1: deep end	255 kNm	775 kNm	265 kNm	775 kNm
2: quarter span	133 kNm	499 kNm	199 kNm	592 kNm
3: half span	3,42 kNm	322 kNm	132 kNm	425 kNm
4: three quarters	< 0	322 kNm	66,2 kNm	273 kNm
5: shallow end	< 0	322 kNm	0	140 kNm
$\left(M_{c,Rd} / M_{Sd}\right)_{\min}$	3,05		2,93	
μ_{SE}	< 0		< 0	
m_t	0,296		0,810	

Slenderness is calculated as

For beam $\lambda = \frac{L_{beam}/i_{z,C1}}{\sqrt{\alpha + \frac{I_{t,C1}L_{beam}^2}{2{,}6\pi^2 I_{z,C1} i_0^2}}} = 160{,}7$, where $\alpha = \frac{e_{z,A}^2 + I_{w,C1}/I_{z,C1}}{i_0^2} = 1{,}269$

Column $\lambda = \frac{L_{beam}/i_{z,C2}}{\sqrt{\alpha + \frac{I_{t,C2}L_{column}^2}{2{,}6\pi^2 I_{z,C2} i_0^2}}} = 92{,}8$, where $\alpha = \frac{e_{z,D}^2 + I_{w,C2}/I_{z,C2}}{i_0^2} = 1{,}366$

Relative slenderness

For beam: $\bar{\lambda}_{LT} = c\sqrt{m_t}\sqrt{\frac{W_{y,C1}}{A_{C1}} \cdot \frac{2e_{z,A}}{i_0^2}}\lambda = 0.943$

For column: $\bar{\lambda}_{LT} = c\sqrt{m_t}\sqrt{\frac{W_{y,C2}}{A_{C2}} \cdot \frac{2e_{z,D}}{i_0^2}}\lambda = 1.167$ *

* Note: Because $\bar{\lambda}_{LT} \geq 1{,}0$ we can try using $c = 1{,}0$ and $e_{z,C2}$ but in that case $\bar{\lambda}_{LT} = 0{,}886$ making calculation unconservative.

Critical moments are:

For beam: $M_{cr} = \left(\frac{1}{m_t c^2}\right) M_{cr0} = 872\ kNm$,

where $M_{cr0} = \left(\frac{i_0^2}{2e_{z,C1}}\right) N_{cr,TFB} = 292\ kNm$.

For column: $M_{cr} = \left(\frac{1}{m_t c^2}\right) M_{cr0} = 569\ kNm$,

where $M_{cr0} = \left(\frac{i_0^2}{2e_{z,C2}}\right) N_{cr,TFB} = 936\ kNm$.

Reduction factors

Reduction factors are calculated for in-plane and out-of-plane axial resistance reduction and for bending capacity reduction in lateral torsional buckling.

$\chi = \frac{1}{\phi + \sqrt{\phi^2 - \bar{\lambda}^2}}$, where

$\phi = 0{,}5\left[1 + \alpha\left(\bar{\lambda} - 0{,}2\right) + \bar{\lambda}^2\right]$

$$\bar{\lambda} = \sqrt{\frac{N_{Rk,\max}}{N_{cr,\min}}} \quad \text{for axial compression}$$

$$\bar{\lambda} = \sqrt{\frac{M_{y,Rk,\max}}{M_{cr,\min}}} \quad \text{for bending}$$

In case of out-of-plane compression and lateral torsional buckling, the minimum reduction factors are used:

	Beam				Column			
	α	$\bar{\lambda}$	ϕ	χ	α	$\bar{\lambda}$	ϕ	χ
FBy	0.34	0.482	0.664	0.892	0.34	0.312	0.568	0.960
FBz, TF, TFB	0.49	1.697	2.307	0.258	0.49	0.903	1.080	0.598
LTB	0.76	0.943	1.227	0.497	0.76	1.168	1.549	0.389

Interaction factors

$$k_{yy} = \min\left[C_{my}\left(1+0{,}6\bar{\lambda}_y \frac{N_{Ed}}{\chi_y N_{Rk}/\gamma_{M1}}\right); C_{my}\left(1+0{,}6\frac{N_{Ed}}{\chi_y N_{Rk}/\gamma_{M1}}\right)\right] \text{ and}$$

$$k_{zy} = \max\left[1-\frac{0{,}05\bar{\lambda}_z}{(C_{mLT}-0{,}25)}\frac{N_{Ed}}{\chi_z N_{Rk}/\gamma_{M1}}; 1-\frac{0{,}05}{(C_{mLT}-0{,}25)}\frac{N_{Ed}}{\chi_z N_{Rk}/\gamma_{M1}}\right].$$

Equivalent uniform moment factors are

$C_{my} = 0{,}9$

$C_{mLT} = \max(0{,}6+0{,}4\psi\,;\,0{,}4)$ for columns

$C_{mLT} = \max(0{,}2+0{,}8\alpha_S\,;\,0{,}4)$ for beams where $\alpha_S \geq 0$

$C_{mLT} = \max(0{,}1-0{,}8\alpha_S\,;\,0{,}4)$ for beams where $\alpha_S < 0$ and $\psi \geq 0$

$C_{mLT} = \max[0{,}1(1-\psi)-0{,}8\alpha_S\,;\,0{,}4]$ for beams where $\alpha_S < 0$ and $\psi < 0$

Moment distribution factors are

$\psi = M_{y,Ed,1}/M_{y,Ed,5}$

$\alpha_S = M_{y,Ed,3}/M_{y,Ed,5}$

	Interaction factors	
	k_{yy}	k_{zy}
A: beam apex	0.907	0.969
B: beam constant part	0.99	0.965
C_1: beam corner	0.907	0.970
C_2: column corner	0.906	0.993
D: column support	0.910	0.988

Limit states conditions

Members subjected to combined bending and axial compression shall satisfy ULS conditions expressed in EC3 as interaction formulae (EN 1993-1-1, 6.3.3):

	$\frac{N_{Ed}}{\chi_y N_{Rk}/\gamma_{M1}} + k_{yy}\frac{M_{y,Ed}}{\chi_{LT} M_{y,Rk}/\gamma_{M1}}$	$\frac{N_{Ed}}{\chi_z N_{Rk}/\gamma_{M1}} + k_{zy}\frac{M_{y,Ed}}{\chi_{LT} M_{y,Rk}/\gamma_{M1}}$	$\frac{V_{z,Ed}}{V_{z,Rk}/\gamma_{M0}}$
A: beam apex	0.549	0.651	0.018
B: beam	0.388	0.491	0.115
C_1: beam	0.630	0.736	0.085
C_2: column	0.833	**0.930**	0.056
D: column	0.057	0.091	0.219

For SLS the maximum of vertical deflection of a beam cannot exceed 1/200 of the span and the horizontal deflection of the column 1/100 of its height.

	vertical deflection $u_{\lim} = 100\ mm$	horizontal deflection $v_{\lim} = 60\ mm$
A: beam apex	**33.5 mm**	0.4 mm
B: beam constant part	10.5 mm	3.7 mm
C_1: beam corner	0.6 mm	6.5 mm
C_2: column corner	0.6 mm	**7.7 mm**
D: column support	0.0 mm	0.0 m

Assuming linear elastic behaviour, predicted load-carrying capacities are

$P_{uls} = 1761\ N/mm^2$

$P_{sls} = 3410\ N/mm^2$